

# Individualized Prediction Bands in Causal Inference with Continuous Treatments

Max Sampson <sup>\*</sup>

Department of Statistics and Actuarial Science, University of Iowa  
and

Kung-Sik Chan

Department of Statistics and Actuarial Science, University of Iowa

November 20, 2025

## Abstract

Individualized treatments are crucial for optimal decision making and treatment allocation, specifically in personalized medicine based on the estimation of an individual's dose-response curve across a continuum of treatment levels, e.g., drug dosage. Current works focus on conditional mean and median estimates, which are useful but do not provide the full picture. We propose viewing causal inference with a continuous treatment as a covariate shift. This allows us to leverage existing weighted conformal prediction methods with both quantile and point estimates to compute individualized uncertainty quantification for dose-response curves. Our method, individualized prediction bands (IPB), is demonstrated via simulations and a real data analysis, which demonstrates the additional medical expenditure caused by continued smoking for selected individuals. The results demonstrate that IPB provides an effective solution to a gap in individual dose-response uncertainty quantification literature.

*Keywords:* Causal Inference; Continuous Treatments; Conformal Prediction; Individualized Medicine; Uncertainty Quantification.

---

<sup>\*</sup>Max Sampson was supported by National Institutes of Health Predoctoral Training Grant T32 HL 144461.

# 1 Introduction

Throughout this paper we focus on the potential outcome framework (Neyman, 1923; Rubin, 1978) with a continuous treatment (Hirano & Imbens, 2004; G. Imbens, 2000). With  $n$  subjects, denote the continuous treatment by  $T_i \in \mathcal{T} = [t_{\min}, t_{\max}]$ ,  $\mathcal{Y}_i = \{Y_i(t) : t \in \mathcal{T}\}$ , the potential outcome at treatment  $t$ , and  $\mathbf{X}_i$ , a vector of  $p$  covariates. Note, the potential outcome for the  $i$ th individual at treatment level  $t$ ,  $Y_i(t)$ , is different than the observed response,  $Y_i$ .  $Y_i(t)$  is what the response for the  $i$ th individual would have been if their treatment was  $t$  and not  $T_i$ .

For example,  $T$  is the time from the onset of hearing loss to a cochlear implant,  $X$  is the gender (which we assume is the only variable that directly affects the treatment and the response), and  $Y$  is a measure of hearing function. It is of interest to find the time window for a cochlear implant to “recover” a certain level of hearing function. That is, what is a realistic value of time after hearing loss,  $t$ , so that  $Y(t)$  is as large as possible. Another example is  $T$  is the average yearly smoking load,  $\mathbf{X}$  demographic and socioeconomic variables, and  $Y$  the subject’s medical costs over a certain period. The problem is to assess how much of the medical costs were directly caused by smoking vs not smoking,  $Y_i - Y_i(0)$ . These questions are important on a population level, what is the optimal average time window for a cochlear implant? They are also very important on an individual level, what is the optimal time window for this specific patient to receive a cochlear implant? These questions can be answered with counterfactual dose-response functions, which we break up into population level average dose-response functions,

$$\mu(t) = E(Y(t)),$$

conditional average dose-response functions,

$$\mu(t \mid \mathbf{X}) = E(Y(t) \mid \mathbf{X}),$$

and individual dose-response functions,

$$Y_i(t) \mid \mathbf{X}_i.$$

In this paper we focus on the later, individual dose-response functions. In the remainder of the introduction, we introduce the notational and ideological framework of our problem, as well as useful background information. In Section 2 we discuss existing methods that form causal prediction intervals and bands for individuals when the treatment is continuous, as well as formally introduce our method, Individualized Prediction Bands (IPB). We then demonstrate the usefulness of IPB via numerical experiments and a real application which looks at the economic benefits quitting smoking can have in Section 3.

## 1.1 Causal Inference Assumptions

For a causal statement to be made using dose-response functions, as in the case with a binary/discrete treatment, we need certain assumptions. Following Rosenbaum and Rubin, 1983, 1984, Lechner, 2001, and Schwab, Linhardt, Bauer, et al., 2020, we assume unconfoundedness, positivity, and the stable unit treatment value assumption (SUTVA). Strong unconfoundedness is the assumption that the treatment is independent of all potential outcomes conditional on  $\mathbf{X}$ . That is, any relationship between potential outcomes and the treatment can be explained by measured covariates. The assumption written out is

$$\mathcal{Y} \perp\!\!\!\perp T \mid \mathbf{X}.$$

Strong unconfoundedness implies that all confounders have been measured and are present in  $\mathbf{X}$ . Weak unconfoundedness is sometimes assumed instead, for example in Hirano and Imbens, 2004; G. Imbens, 2000. Weak unconfoundedness is the assumption that the treatment is independent of each potential outcome conditional on  $\mathbf{X}$ , instead of independent of all potential outcomes.

Positivity, or the common support assumption, is the assumption that it must be possible to observe all possible treatment levels with a probability greater than zero. With a discrete number of treatments positivity is

$$0 < P(T = t \mid \mathbf{X}) < 1 \text{ a.s.}, \forall t \in \{t_1, \dots, t_m\}.$$

In the continuous treatment case, positivity is

$$P(T \in \mathcal{A} \mid \mathbf{X}) > 0 \text{ a.s.}, \text{ for every measurable set } \mathcal{A} \in \mathcal{T} \text{ with positive Lebesgue measure}$$

(Imai & van Dyk, 2004). Positivity can be further broken up into two types of positivity. Deterministic positivity, that it is possible for any individual to receive any treatment, and random positivity, that in the observed sample individuals with similar covariates have received multiple values of a treatment (Westreich & Cole, 2010).

The assumption of SUTVA has two parts. The first part is no interference. That is, the treatment assigned to one individual will not affect the outcome of another individual. The second part is consistency. Consistency requires the treatment to be well defined, so there is only one version of each treatment value. For example, taking a new drug to reduce fevers means the pills contain exactly the same dosage at each dose level (Rosenbaum & Rubin, 1983, 1984). SUTVA implies that the observed response can be written as the counterfactual of the observed treatment,  $Y_i = Y_i(T_i)$ . These assumptions will be implicitly made throughout the paper.

## 1.2 Traditional Inferential Targets

The majority of existing methods in causal inference with continuous treatments focus on the average dose-response curve for a population or a subset of the population. There has been some work done on average dose-response functions using both parametric methods and non-parametric methods (Flores, Flores-Lagunes, Gonzalez, & Neumann, 2012; J. L. Hill, 2011; Hirano & Imbens, 2004; Imai & van Dyk, 2004; G. Imbens, 2000; Zhao, van

Dyk, & Imai, 2020), as well as works that have studied the conditional and individual dose-response function (G. W. Imbens & Wooldridge, 2009; Schwab, Linhardt, Bauer, et al., 2020; Shalit, Johansson, & Sontag, 2016).

The methods that investigate individual dose-response functions lack reliable uncertainty estimates. One solution to this for general regression problems with a continuous response has been to use quantile regression Koenker and Bassett, 1978. This has been used to estimate the conditional quantile treatment effect (CQTE) in causal inference (Fort, 2016). In the binary case, the CQTE is defined as the difference of the  $\beta$ -th quantiles between  $Y(1)$  and  $Y(0)$  conditioned on  $\mathbf{X} = \mathbf{x}$ . Though, reliable uncertainty estimates are still needed for CQTE as well as quantile regression done with continuous treatments.

Motivated by the question of: What is the best intervention window for an individual to receive a treatment? We consider the problem of estimating conditional quantiles of the individual dose-response function. We propose to do this in two ways, both of which only require observational data. The first is constructing conformal prediction bands about the conditional average dose-response function. The second is using conformal prediction to adjust conditional quantiles to form prediction bands. To form these individualized prediction bands, we view observational causal inference with a continuous treatment as a covariate shift.

### 1.3 Counterfactuals and Covariate Shift

One way to view counterfactual inference is as a question: “What if the treatment was applied according to a distribution independent of confounders?” This question is important to keep in mind when constructing estimates for  $Y(t)$ ,  $t \in \mathcal{T}$  using the observed i.i.d. observations,  $(Y_i^{obs}, T_i)$ . Consider a simple example of how sugar consumption affects heart disease. A person who consumes a lot of sugar may be less likely to exercise regularly than someone who is health conscious and does not consume a lot of sugar. If we ignore the

amount someone exercises, our causal estimate of sugar consumption on heart health will be biased. If we control for how often a person exercises, along with all other variables that affect both how often a person consumes sugar and their heart health, we would be able to estimate the causal effect of sugar on heart disease, and how changes in sugar consumption can causally effect heart disease.

To conduct counterfactual inference, we can view the observed distribution as

$$(Y_i, T_i, \mathbf{X}_i) \stackrel{i.i.d.}{\sim} P_{\mathbf{X}} \times P_{T|\mathbf{X}} \times P_{Y|\mathbf{X}, T}, \quad i = 1, 2, \dots, n,$$

where  $P$  and  $P_{\cdot| \cdot}$  denote the marginal probability distribution and the conditional probability distribution, respectively. The treatment being assigned independently of confounders, as is the case in randomized experiments, can be viewed as a covariate shift from our original distribution:

$$(Y_i, T_i, \mathbf{X}_i) \stackrel{i.i.d.}{\sim} P_{\mathbf{X}} \times Q_T \times P_{Y|\mathbf{X}, T}, \quad i = n+1, n+2, \dots,$$

where  $Q_T$  is the new distribution of  $T$  after the shift has occurred, for instance, the observed marginal distribution of  $T$ , and the conditional distribution,  $P_{Y|\mathbf{X}, T}$ , and marginal distribution,  $P_{\mathbf{X}}$ , remain the same. For example, what would the effect on hearing be if we gave someone a cochlear implant quickly after hearing loss began, as opposed to several years later, assuming all else is equal.

This will allow us to infer what happens when the treatment is assigned independently of any covariates. Point estimates for covariate shifts have been widely studied in machine learning (Shimodaira, 2000). Interval (both confidence and prediction intervals) estimates are, however, understudied in the literature. Weighted conformal inference has recently allowed prediction intervals to be created from data with known covariate shifts (Tibshirani, Foygel Barber, Candes, & Ramdas, 2019) and unknown, but estimated, covariate shifts (L. Lei & Candès, 2021).

We combine the idea of viewing causal inference with a continuous treatment as a

covariate shift with conformal prediction to form individual prediction bands to answer the question, “What if the treatment was assigned independently of the confounders?”

## 1.4 Conformal Prediction

Conformal prediction is a general method of creating prediction intervals that provide a non-asymptotic, distribution free coverage guarantee. We focus on using split conformal prediction to form prediction bands.

Split conformal prediction has three steps. The first is to split the data into a training set,  $Z_{tr}$ , and a calibration set,  $Z_{cal}$ . The second step trains a model on the training set. The model chosen depends on what non-conformity score one chooses to work with. For a continuous response, conditional mean and quantile regression models are common choices (J. Lei, G’Sell, Rinaldo, et al., 2018; Romano, Patterson, & Candes, 2019; Vovk, Gammerman, & Shafer, 2005). The third step computes the non-conformity scores on the calibration data. A common non-conformity score for a regression problem is the absolute difference,  $V_i = |Y_i - \hat{f}(\mathbf{X}_i)|$  (Papadopoulos, Proedrou, Vovk, & Gammerman, 2002). The prediction interval that is output will depend on the non-conformity score used, in the case of the absolute difference the interval is

$$C(\mathbf{X}_{n+1}) = [\hat{f}(\mathbf{X}_{n+1}) - Q_{1-\alpha}(\mathbf{V}; Z_{cal}), \hat{f}(\mathbf{X}_{n+1}) + Q_{1-\alpha}(\mathbf{V}; Z_{cal})],$$

where

$$Q_{1-\alpha}(\mathbf{V}; Z_{cal}) := (1 - \alpha)(1 + \frac{1}{|Z_{cal}|}) - \text{th empirical quantile of } \{V_i\},$$

and  $|Z_{cal}|$  is the size of the calibration set. The process of split conformal prediction described above is formalized in Algorithm 1.

---

**Algorithm 1:** Split Conformal Prediction

---

**Input:** Significance level  $\alpha$ , dataset  $\mathcal{Z} = \{(Y_i, \mathbf{X}_i)\}_{i \in \mathcal{I}}$ , test point  $\mathbf{x}$ , and regression algorithm  $f(\mathbf{X}; \mathcal{D})$

**Output:** Prediction interval  $\hat{C}(\mathbf{x})$

**1 Procedure**

- 2 Split  $\mathcal{Z}$  into a training set  $\mathcal{Z}_{tr} = \{(Y_i, \mathbf{X}_i)\}_{i \in \mathcal{I}_{tr}}$  and a calibration set  $\mathcal{Z}_{cal} = \{(Y_i, \mathbf{X}_i)\}_{i \in \mathcal{I}_{cal}}$ ;
- 3 Train the model  $\hat{f}(\mathbf{x}; \mathcal{Z}_{tr})$  using the training set;
- 4 **foreach**  $i \in \mathcal{I}_{cal}$  **do**
- 5     Compute score  $V_i = |\hat{f}(\mathbf{X}_i; \mathcal{Z}_{tr}) - Y_i|$ ;
- 6     Compute  $\eta(\mathbf{x})$  as the  $(1 - \alpha)$ -quantile of the scores  $\{V_i\}$ ;
- 7 **return**  $\hat{C}(\mathbf{x}) = [\hat{f}(\mathbf{x}; \mathcal{Z}_{tr}) - \eta(\mathbf{x}), \hat{f}(\mathbf{x}; \mathcal{Z}_{tr}) + \eta(\mathbf{x})]$

---

Conformal prediction can also be used with conditional quantile regression (L. Lei & Candès, 2021; Romano, Patterson, & Candes, 2019). The steps are the same as with a point estimate, except the trained model is used to estimate lower and upper conditional quantiles,  $\hat{q}_{\alpha_{low}}$  and  $\hat{q}_{\alpha_{high}}$ . The non-conformity scores are then,  $V_i = \max\{\hat{q}_{\alpha_{low}}(\mathbf{X}_i) - Y_i, Y_i - \hat{q}_{\alpha_{high}}(\mathbf{X}_i)\}$ . Finally, for the new input,  $\mathbf{X}_{n+1}$ , the prediction interval for  $Y_{n+1}$  is

$$C(\mathbf{X}_{n+1}) = [\hat{q}_{\alpha_{low}}(\mathbf{X}_{n+1}) - Q_{1-\alpha}(\mathbf{V}; \mathcal{Z}_{cal}), \hat{q}_{\alpha_{high}} + Q_{1-\alpha}(\mathbf{V}; \mathcal{Z}_{cal})]$$

where

$$Q_{1-\alpha}(\mathbf{V}; \mathcal{Z}_{cal}) := (1 - \alpha)(1 + \frac{1}{|\mathcal{Z}_{cal}|}) - \text{th empirical quantile of } \{V_i\}.$$

We focus on conformal prediction with quantile regression with IPB, as it inherits some nice doubly robust properties first established in L. Lei and Candès, 2021. The doubly robust property provides a coverage guarantee when either the conditional distribution of the treatment, conditional quantile outcome regression model, or both are correctly specified. We also provide a method to form individualized prediction bands that starts with a point estimate. The main idea of the next section is that the non-conformity scores

can be shifted to form prediction intervals when covariate shifts occur. So, by viewing the causal inference problem as a covariate shift, we can leverage weighted conformal prediction to form individual prediction bands.

## 1.5 Weighted Conformal Inference

Our goal is to shift the treatment distribution from being drawn from the conditional distribution of  $T | \mathbf{X}$  to being drawn from an assignment distribution that does not depend on confounders, for example the marginal treatment distribution  $f_T$ . To do this, following L. Lei and Candès, 2021; Tibshirani, Foygel Barber, Candes, and Ramdas, 2019, we need to look at the likelihood ratio of the shifted distributions to find the weight. Similar to importance sampling, the distribution of interest is in the numerator and the observed distribution is in the denominator.

$$\frac{dQ_{T,\mathbf{X}}}{dP_{T,\mathbf{X}}} = \frac{f_{\mathbf{X}}f_T}{f_{\mathbf{X}}f_{T|\mathbf{X}}} = \frac{f_T}{f_{T|\mathbf{X}}} \quad (1)$$

For a continuous treatment, this is the same as the stabilized weights introduced in Robins, Hernán, and Brumback, 2000. This ratio is the same as in the setting of a binary treatment in L. Lei and Candès, 2021, though in our setting with a continuous treatment, we are unable to group treatments together to ignore the marginal distribution like we can in the binary case (L. Lei & Candès, 2021). Instead of directly using the marginal distribution in the numerator of the weight, we use an assignment distribution. The assignment or intervention distribution is the distribution by which the treatment is assigned. This provides the flexibility to ask questions such as, “what if we truncate possible values of the treatment” or “what if we don’t randomly assign the treatment, but assign it conditionally on observed covariates in a specific way”. The conditional distribution of a continuous treatment is known as the generalized propensity score (GPS), and is commonly used in causal inference with continuous treatments. A more detailed discussion of the GPS and

its use in causal inference with continuous treatments can be found in Appendix D of the supplementary materials. Our focus is on combining the GPS with an outcome regression model to form individualized prediction bands. For a discussion of estimating the GPS, see Tu, 2019 who recommends a gradient boosting approach in practice.

## 1.6 Outcome Regression Models

Outcome regression models are commonly used to model the conditional mean of the response,  $Y$ , given the variables,  $\mathbf{X}$ , that are necessary to satisfy the strong ignorability assumption along with the treatment,  $T$  (Hernán & Robins, 2020). For example, if the treatment and covariates are linearly related to the response, one could use ordinary least squares to estimate  $\beta_0$ ,  $\beta_1$ , and  $\beta_2$  in the equation below.

$$E(Y | T, \mathbf{X}) = \beta_0 + \beta_1 T + \beta_2 \mathbf{X}$$

If the model is correctly specified, it can be used to make causal claims, assuming that all causal assumptions (e.g., unconfoundedness, positivity, etc) are true. This is true because the assumption of consistency tells us that the conditional expectation of a potential outcome at a given treatment level is the same as the observed response given the treatment level. That is,  $E(Y(t) | T = t, \mathbf{X}) = E(Y | T = t, \mathbf{X})$ . J. L. Hill, 2011 used this approach with Bayesian Additive Regression Trees to look at population level comparisons between treatments.

This idea can be extended beyond the conditional mean if we use a stronger form of consistency. Using this consistency assumption with strong ignorability, we can show that a properly specified outcome regression model can tell us about the potential outcome,

$$\begin{aligned} Y(t) | \mathbf{X} \\ \stackrel{d}{=} Y(t) | \mathbf{X}, T = t \\ \stackrel{d}{=} Y | \mathbf{X}, T = t, \end{aligned}$$

where the first equality is by the strong ignorability assumption and the second equality is by the stronger consistency assumption. This brief explanation tells us that if we are able to model the conditional distribution of  $Y | \mathbf{X}, T$  correctly, we can use it to make valid causal claims.

We are not the first to make the argument that outcome regression models can be extended beyond the conditional mean. Zhang, Chen, Troendle, and Zhang, 2012 argue that for population causal effects, such as the average treatment effect, the median may be a better measure than the mean for heavily skewed distributions. This can be generalized to quantiles other than the median. For example, Fort, 2016 looked at the conditional quantiles to estimate conditional quantile treatment effects.

We build on these approaches by combining conditional quantile regression with weighted conformal prediction in IPB. Combining conditional quantile regression with weighted conformal prediction provides us robustness against misspecified conditional quantile models, and has a negligible impact when the conditional model is correctly specified.

## 2 Methods

### 2.1 Existing Methods

To our knowledge, there are two existing methods that combine conformal prediction and causal inference with a continuous treatment. The first, Schröder, Frauen, Schweisthal, et al., 2025, focuses on creating prediction intervals for causal effects, e.g.  $Y(t^*) - Y(t)$ , and not the dose-response curve as we do. The second, Verhaeghe, Jonkers, and Van Hoecke, 2024, is more comparable to our approach because they create prediction intervals and bands for the dose-response curve. We outline the key differences between our approach and their approach below.

The first difference between our approach and that found in Verhaeghe, Jonkers, and

Van Hoecke, 2024 is that our method can utilize a conditional quantile model as the outcome model, giving our dose-response prediction intervals an asymptotic doubly robust property, that the coverage is guaranteed when either the outcome model or the generalized propensity model is correctly specified.

The second difference between our approaches is that they restrict the treatment intervention assignment to be uniform over the treatment values. We demonstrate numerically in Appendix B of the supplementary materials that if the treatment intervention assignment is not uniform, but a uniform weight is used, then the resulting average coverage of the prediction intervals is similar to our approach, but is more variable. This is consistent with the results seen when computing treatment effects from observational data, unstabilized weights (those which use 1 in the numerator instead of the marginal distribution) lead to estimates with higher variability (Imai & Ratkovic, 2015).

They also propose a second weight for the scores that is a modified version of the kernel density weight found in Tibshirani, Foygel Barber, Candes, and Ramdas, 2019 to have better treatment conditional coverage,

$$w(\mathbf{X}_i, T_i) = \frac{\mathbb{1}(T_i \in [t_{\min}, t_{\max}]) \times K(\frac{T_i - t}{h})}{f_{T|\mathbf{X}}(T_i \mid \mathbf{X}_i)},$$

where  $K$  is a kernel density and  $h$  its bandwidth. This is done to attempt to improve the conditional coverage for a given treatment. One problem with this approach is that the kernel density estimates need to be computed and stored for each value of  $t$  a practitioner plans to investigate.

We note that this approach is a special case of by IPB, where the kernel density estimator serves as the treatment assignment model. We believe an approach that is as good, if not better, in this situation is using IPB with a known distribution that puts a majority of its mass near the treatment of interest,  $t$ , instead of a kernel density estimation near  $t$ . This is more flexible than a kernel density estimator because it can be a truncated distribution, or a heavily skewed distribution if the treatment of interest is near the boundary

of possible treatment values. Also, assuming that the quantile model used with IPB is well calibrated, IPB provides conditional or near conditional coverage, making this weighted approach less necessary. Tibshirani, Foygel Barber, Candes, and Ramdas, 2019 used this approach because they looked at a  $d$ -dimensional predictor where specifying such a specific distribution would have been more difficult. Because the treatment is assumed to be univariate, though IPB and the methods presented in Verhaeghe, Jonkers, and Van Hoecke, 2024 can be generalized to multiple treatments, other approaches can be taken to ensure near treatment conditional coverage.

## 2.2 Individual Prediction Bands with Continuous Treatments

We outline our method, Individual Prediction Bands with Continuous Treatments (IPB), below. IPB combines the outcome regression model for a continuous treatment with the generalized propensity score for individual causal predictions to form individual doubly robust prediction intervals, as well as individual dose-response prediction bands.

On its own, looking at a prediction interval for a treatment drawn from the marginal distribution may not be of much interest. We're more likely to be interested in what happens if we assign a specific treatment, or treatments in a small interval near each other. Instead of letting  $dQ_{T,\mathbf{X}} = f_{\mathbf{X}} f_T$ , let  $dQ_{T,\mathbf{X}} = f_{\mathbf{X}} h_T$  where  $h_T$  has no reliance on  $\mathbf{X}$  and has a more concentrated density near some point,  $t$ , than  $f_T$ . Generally,  $h_t$  is known and is henceforth known as the intervention or treatment assignment distribution. To motivate this idea, consider the following example.

Imagine a person tears their ACL and their doctor wants to know what the optimal waiting time is for their surgery. They decide that the best time to give the surgery is two weeks after the injury has occurred so the individual is able to let the swelling reduce, a common approach for ACL tears (Shen, Liu, Xu, et al., 2022). Because of the surgeon's schedule, the surgery cannot always be scheduled exactly two weeks from the injury. There

also may be times when the swelling does not go down, and the surgery needs to be postponed for a few days (Shen, Liu, Xu, et al., 2022). So, we would like to create a prediction set that gives a high likelihood of receiving the surgery around two weeks after injury, but that has positive probability for that individual to receive the surgery at a later time because of unforeseen complications. This idea is further explored numerically in Section 3.1.1.

Over all treatment values, we are interested in creating a prediction interval with coverage guarantees. Our observed sample data do not match the data we wish to predict because we are not observing a natural treatment based on a set of covariates. This was addressed by Tibshirani, Foygel Barber, Candes, and Ramdas, 2019 by introducing a weighted version on conformal inference with a known likelihood ratio,

$$w(\cdot) = \frac{dQ}{dP}(\cdot).$$

Herein and henceforth,  $\frac{dQ}{dP}$  is given by (1) with  $f_T$  replaced by  $h_T$ . This idea was further extended in L. Lei and Candès, 2021 to the scenario where the likelihood ratio was unknown. They specifically looked at a binary treatment with quantile regression modeling the response. We extend this to a continuous treatment with any split conformal method, as well as specifically with split conformal quantile regression.

Algorithm 2 sketches the method for any split conformal method. Algorithm 3 shows the method as applied to split conformal quantile regression, which we use in the majority of our numerical studies. We note that these methods can also use a signed-conformal regression approach to form one-sided prediction intervals (Linusson, Johansson, & Löfström, 2014; Romano, Patterson, & Candes, 2019). These algorithms can be viewed as weighting the scores in conformal prediction, similar to importance weighting of the response done with other causal inference methods.

The weights we use are,

$$W_i = \hat{w}(\mathbf{X}_i, T_i; Z_{tr}) = \frac{h_T(T_i)}{\hat{f}_{T|\mathbf{X}}(T_i \mid \mathbf{X}_i)} \quad \forall i \in \mathcal{I}_{cal},$$

where  $\hat{\cdot}$  represents an a quantity estimated on the training set.

---

**Algorithm 2:** Weighted Conformal Point Regression

---

**Input:** Significance level  $\alpha$ , dataset  $\mathcal{Z} = \{(Y_i, T_i, \mathbf{X}_i)\}_{i \in \mathcal{I}}$ , test point  $(\mathbf{x}, t)$ ,

regression algorithm  $f(\mathbf{X}, t; \mathcal{D})$ , weight function  $\hat{w}(\mathbf{x}, t; \mathcal{D})$

**Output:** Prediction interval  $\hat{C}(\mathbf{x}, t)$

**1 Procedure**

**2** Split  $\mathcal{Z}$  into a training set  $\mathcal{Z}_{tr} = \{(Y_i, T_i, \mathbf{X}_i)\}_{i \in \mathcal{I}_{tr}}$  and a calibration set

$\mathcal{Z}_{cal} = \{(Y_i, T_i, \mathbf{X}_i)\}_{i \in \mathcal{I}_{cal}}$ ;

**3** Train the model  $\hat{f}(\mathbf{x}, t; \mathcal{Z}_{tr})$  using the training set;

**4 foreach**  $i \in \mathcal{I}_{cal}$  **do**

**5** Compute score  $V_i = |\hat{f}(\mathbf{X}_i, T_i; \mathcal{Z}_{tr}) - Y_i|$ ;

**6** Compute weight  $W_i = \hat{w}(\mathbf{X}_i, T_i; \mathcal{Z}_{tr})$ ;

**7** Normalize weights::;

$$\hat{p}_i(\mathbf{x}, t) = \frac{W_i}{\sum_{j \in \mathcal{I}_{cal}} W_j + \hat{w}(\mathbf{x}, t; \mathcal{Z}_{tr})};$$

$$\hat{p}_\infty(\mathbf{x}, t) = \frac{\hat{w}(\mathbf{x}, t; \mathcal{Z}_{tr})}{\sum_{j \in \mathcal{I}_{cal}} W_j + \hat{w}(\mathbf{x}, t; \mathcal{Z}_{tr})};$$

**10** Compute  $\eta(\mathbf{x}, t)$  as the  $(1 - \alpha)$ -quantile of the distribution

$\sum_{i \in \mathcal{I}_{cal}} \hat{p}_i(\mathbf{x}, t) \delta_{V_i} + \hat{p}_\infty(\mathbf{x}, t) \delta_\infty$ , where  $\delta$  is the Dirac delta function;

**11 return**  $\hat{C}(\mathbf{x}, t) = [\hat{f}(\mathbf{x}, t; \mathcal{Z}_{tr}) - \eta(\mathbf{x}, t), \hat{f}(\mathbf{x}, t; \mathcal{Z}_{tr}) + \eta(\mathbf{x}, t)]$

---

If the weights are known, marginal coverage for a population with a treatment that has been assigned according to  $Q_T$  is guaranteed. Below we state the theoretical guarantees of these algorithms, which are direct results from L. Lei and Candès, 2021. Algorithm 4 describes how to create a prediction band for the dose-response curve. This can be used for continuous treatments, as well as multi-class treatments.

Proposition 1. Consider Algorithm 3. Assume  $(\mathbf{X}_i, T_i, Y_i) \stackrel{iid}{\sim} P_{T|\mathbf{X}} \times P_{\mathbf{X}} \times P_{Y|\mathbf{X}, T}$  and  $w(\cdot) = \frac{dQ_T}{dQ_{T|\mathbf{X}}}(\cdot)$ .

---

**Algorithm 3:** Weighted Conformal Quantile Regression

---

**Input:** Significance level  $\alpha$ , dataset  $\mathcal{Z} = \{(Y_i, T_i, \mathbf{X}_i)\}_{i \in \mathcal{I}}$ , test point  $(\mathbf{x}, t)$ , quantile regression algorithm  $q_\beta(\mathbf{X}, t; \mathcal{D})$ , weight function  $\hat{w}(\mathbf{x}, t; \mathcal{D})$

**Output:** Prediction interval  $\hat{C}(\mathbf{x}, t)$

**1 Procedure**

2     Split  $\mathcal{Z}$  into a training set  $\mathcal{Z}_{tr} = \{(Y_i, T_i, \mathbf{X}_i)\}_{i \in \mathcal{I}_{tr}}$  and a calibration set  $\mathcal{Z}_{cal} = \{(Y_i, T_i, \mathbf{X}_i)\}_{i \in \mathcal{I}_{cal}}$ ;

3     Train the quantile models  $\hat{q}_{\alpha_{low}}(\mathbf{x}, t; \mathcal{Z}_{tr})$  and  $\hat{q}_{\alpha_{high}}(\mathbf{x}, t; \mathcal{Z}_{tr})$ ;

4     **foreach**  $i \in \mathcal{I}_{cal}$  **do**

5         Compute score  $V_i = \max \{\hat{q}_{\alpha_{low}}(\mathbf{X}_i, T_i; \mathcal{Z}_{tr}) - Y_i, Y_i - \hat{q}_{\alpha_{high}}(\mathbf{X}_i, T_i; \mathcal{Z}_{tr})\}$ ;

6         Compute weight  $W_i = \hat{w}(\mathbf{X}_i, T_i; \mathcal{Z}_{tr})$ ;

7     Normalize weights:;

8      $\hat{p}_i(\mathbf{x}, t) = \frac{W_i}{\sum_{j \in \mathcal{I}_{cal}} W_j + \hat{w}(\mathbf{x}, t; \mathcal{Z}_{tr})}$ ;

9      $\hat{p}_\infty(\mathbf{x}, t) = \frac{\hat{w}(\mathbf{x}, t; \mathcal{Z}_{tr})}{\sum_{j \in \mathcal{I}_{cal}} W_j + \hat{w}(\mathbf{x}, t; \mathcal{Z}_{tr})}$ ;

10    Compute  $\eta(\mathbf{x}, t)$  as the  $(1 - \alpha)$ -quantile of the distribution

11    
$$\sum_{i \in \mathcal{I}_{cal}} \hat{p}_i(\mathbf{x}, t) \delta_{V_i} + \hat{p}_\infty(\mathbf{x}, t) \delta_\infty$$
;

11 **return**  $\hat{C}(\mathbf{x}, t) = [\hat{q}_{\alpha_{low}}(\mathbf{x}, t; \mathcal{Z}_{tr}) - \eta(\mathbf{x}, t), \hat{q}_{\alpha_{high}}(\mathbf{x}, t; \mathcal{Z}_{tr}) + \eta(\mathbf{x}, t)]$

---

1. If  $\hat{w}(\cdot) = w(\cdot)$ , then

$$\mathbb{P}_{(Y,T,\mathbf{X}) \sim P_{\mathbf{X}} \times Q_T \times P_{Y|T,\mathbf{X}}} (Y(T) \in \hat{C}(\mathbf{X}, T)) \geq 1 - \alpha.$$

2. If  $\hat{w}(\cdot) = w(\cdot)$ , the non-conformity scores  $\{V_i : i \in \mathcal{I}_{cal}\}$  have no ties almost surely,  $Q_T$  is absolutely continuous with respect to  $P_{T|\mathbf{X}}$ , and  $(\mathbb{E}_{\mathbf{X},T \sim P_{\mathbf{X}} \times P_{T|\mathbf{X}}} [\hat{w}(X, T)^r])^{1/r} \leq M_r < \infty$  for some constant  $M_r$ , then

$$1 - \alpha \leq \mathbb{P}_{(Y,T,\mathbf{X}) \sim P_{\mathbf{X}} \times Q_T \times P_{Y|T,\mathbf{X}}} (Y(T) \in \hat{C}(\mathbf{X}, T)) \leq 1 - \alpha + cn^{1/r-1},$$

where  $c$  is a positive constant that only depends on  $M_r$  and  $r$ .

In the general case where  $\hat{w}(\cdot) \neq w(\cdot)$ , set  $\Delta_w = \frac{1}{2}\mathbb{E}_{\mathbf{X},T \sim P_{\mathbf{X}} \times P_{T|\mathbf{X}}} |\hat{w}(\mathbf{X}, T) - w(\mathbf{X}, T)|$ . Then, coverage is always lower bounded by  $1 - \alpha - \Delta_w$  and upper bounded by  $1 - \alpha + \Delta_w + cn^{1/r-1}$  under the same assumptions as in 2. Again, this proposition is directly from L. Lei and Candès, 2021, Proposition 1.

The next result is directly from L. Lei and Candès, 2021, Corollary 1.

**Proposition 2.** Denote  $N$  as the size of the training set and  $n$  as the size of the calibration set.

Assume that either A1 or A2 (or both) is satisfied:

**A1:**

$$\lim_{N \rightarrow \infty} \mathbb{E} |\hat{w}(\mathbf{X}, T) - w(\mathbf{X}, T)| = 0,$$

**A2:**

$$(1) \quad \alpha_{\text{high}} - \alpha_{\text{low}} = 1 - \alpha;$$

$$(2) \quad \text{there exist } r, b_1, b_2 > 0 \text{ such that } \mathbb{P}(Y = y \mid \mathbf{X} = \mathbf{x}, T = t) \in [b_1, b_2] \text{ uniformly over all } (\mathbf{x}, t, y) \text{ with } y \in [q_{\alpha_{\text{low}}}(\mathbf{x}, t) - r, q_{\alpha_{\text{low}}}(\mathbf{x}, t) + r] \cup [q_{\alpha_{\text{high}}}(\mathbf{x}, t) - r, q_{\alpha_{\text{high}}}(\mathbf{x}, t) + r];$$

$$(3) \quad \mathbb{P}_{\mathbf{X},T \sim P_{\mathbf{X}} \times P_{T|\mathbf{X}}} (w(X) < \infty) = 1, \text{ and there exist } \delta, M > 0 \text{ such that}$$

$$(\mathbb{E}[\hat{w}(\mathbf{X}, T)^{1+\delta}])^{1/(1+\delta)} \leq M;$$

(4) there exist  $k, \ell > 0$  such that

$$\lim_{N \rightarrow \infty} \mathbb{E}[\hat{w}(\mathbf{X}, T) H_N^k(\mathbf{X}, T)] = \lim_{N \rightarrow \infty} \mathbb{E}[w(\mathbf{X}, T) H_N^\ell(\mathbf{X}, T)] = 0, \text{ where}$$

$$H_N(\mathbf{x}, t) = \max\{|\hat{q}_{\alpha_{\text{low}}, N}(\mathbf{x}, t) - q_{\alpha_{\text{low}}}(\mathbf{x}, t)|, |\hat{q}_{\alpha_{\text{high}}, N}(\mathbf{x}, t) - q_{\alpha_{\text{high}}}(\mathbf{x}, t)|\}.$$

Then,

$$\lim_{N, n \rightarrow \infty} \mathbb{P}_{(Y, T, \mathbf{X}) \sim P_{\mathbf{X}} \times Q_T \times P_{Y|\mathbf{X}, T}}(Y(T) \in \hat{C}(\mathbf{X}, T)) \geq 1 - \alpha.$$

Furthermore, under **A2**, for any  $\epsilon > 0$ ,

$$\lim_{N, n \rightarrow \infty} \mathbb{P}_{T, \mathbf{X} \sim P_{\mathbf{X}} \times Q_T}(\mathbb{P}_{(Y, T, \mathbf{X}) \sim P_{\mathbf{X}} \times Q_T \times P_{Y|\mathbf{X}, T}}(Y(T) \in \hat{C}(\mathbf{X}, T) \mid \mathbf{X}, T) \leq 1 - \alpha - \epsilon) = 0.$$

Proposition 1 implies that with well specified weights, individualized prediction intervals have a coverage that is very close to  $1 - \alpha$ . When the weights are not well specified, the difference between the true coverage and the nominal coverage is bounded by  $\Delta_w$ . We note that, although not stated, this also applies to the methods of Verhaeghe, Jonkers, and Van Hoecke, 2024. Proposition 2 provides the same guarantee, and further establishes that the intervals formed by IPB achieve asymptotic conditional coverage when the conditional quantile model is asymptotically correct.

---

**Algorithm 4:** Individualized Prediction Band

---

**Input:** Significance level  $\alpha$ , dataset  $\mathcal{Z} = \{(Y_i, T_i, \mathbf{X}_i)\}_{i \in \mathcal{I}}$ , test point  $\mathbf{x}$ , regression or quantile algorithm for conditional mean or quantile, weight function  $\hat{w}(\mathbf{x}, t; \mathcal{D})$ , treatment interval  $\mathcal{T} = [t_{\min}, t_{\max}]$ , number of splits  $N$

**Output:** Prediction band  $\hat{C}(\mathbf{x}, \mathcal{T})$

**1 Procedure**

```
2   Split  $\mathcal{T}$  into  $N$  treatment values:  $t_1 = t_{\min}, t_2, \dots, t_N = t_{\max}$ ;  
3   for  $k \leftarrow 1$  to  $N$  do  
4       Apply either Algorithm 2 (Weighted Conformal Point Regression) or  
        Algorithm 3 (Weighted Conformal Quantile Regression) at treatment  $t_k$ ;  
5       Record the prediction interval  $\hat{C}(\mathbf{x}, t_k)$ ;  
6   Combine all prediction intervals  $\{\hat{C}(\mathbf{x}, t_k)\}_{k=1}^N$  into a prediction band  $\hat{C}(\mathbf{x}, \mathcal{T})$ ;  
7 return  $\hat{C}(\mathbf{x}, \mathcal{T})$ 
```

---

These algorithms are extensions of the methods discussed in Tibshirani, Foygel Barber, Candes, and Ramdas, 2019 with a known likelihood ratio,  $w(\cdot)$ , and of methods discussed in L. Lei and Candès, 2021 in the case of an unknown, but estimated likelihood ratio,  $\hat{w}(\cdot)$ . In our case, there are scenarios in which the observed conditional treatment assignment is known, and cases where it needs to be estimated. In both cases, IPB leverages weighted conformal prediction to provide guaranteed coverage prediction bands for individual dose-response curves. These propositions also demonstrate the power of the conformal adjustment: that it improves the coverage when an outcome regression model is misspecified, while maintaining the coverage when the outcome regression model is correctly specified.

## 3 Analyses

### 3.1 Simulation Studies

All numerical analyses were done using the R language (R Core Team, 2023). In the first simulation scenario data were generated as follows,  $X_1 \sim N(1, 1)$ ,  $X_2 \sim N(1, 1)$ ,  $X_3 \sim N(4, 1)$ ,  $T | \mathbf{X} \sim N(X_1 - X_2^2 + 0.5X_3, 20)$ , and  $Y(t) | \mathbf{X} \sim N(X_1 + X_2 + t + X_1^2 + X_2^2 + t^2 + X_1t + X_2t + X_1X_2, 9)$  where the Normal distribution is parameterized via the mean and the variance. A visualization of the treatment and covariate relationships can be seen in Figure 1. In the second simulation scenario, data were generated in the same way except the conditional response, which was generated as,  $Y(t) | \mathbf{X} \sim N(X_1 + 2X_2 + t + 5X_1^2, 9)$ .

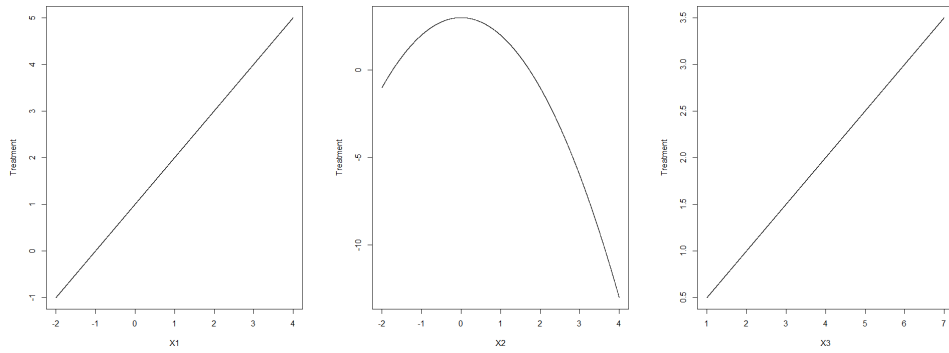


Figure 1: Treatment covariate relationships for simulation setups 1 and 2.

The sample size for each scenario was  $n = 1,000$ . This was split equally between a training set and a calibration set. The simulation size was  $N = 1,000$ . In each simulation, ten out of sample points were generated according to the shifted distribution and used for prediction.

In each simulation, the weights were computed assuming the shifted distribution,  $Q_T$ , was known. For both simulations, there were 5 setups that were considered. The target coverage rate was set to be 90%.

1. Oracle outcome and oracle weight models

2. BART outcome model and oracle weight model
3. Oracle outcome model and estimated weights
4. BART outcome model and estimated weights
5. BART with no adjustment

The oracle outcome model used the true conditional distribution of  $Y(t) \mid \mathbf{X}$  to form the unconformalized quantiles. The Bayesian Additive Regression Trees (BART) outcome model used the 5th and 95th percentiles of the posterior predictive distribution, which was constructed from 2,000 MCMC samples computed using the *dbarts* R package (Dorie, Chipman, & McCulloch, 2025). Letting  $Y_i$  denote the observed response, the BART model for regression assumes the form,

$$Y_i = f(\mathbf{X}_i, T_i) + \epsilon_i, \quad \epsilon_i \stackrel{i.i.d.}{\sim} N(0, \sigma^2),$$

where  $f$  is represented by the sum of  $m$  regression trees,

$$f(\mathbf{x}, t) = g(\mathbf{x}, t; T_1, M_1) + \cdots + g(\mathbf{x}, t; T_m, M_m),$$

where  $T$  is the tree structure and  $M$  is the terminal node. Typically inference with BART is done through MCMC by placing priors on the parameters in the model (Chipman, George, & McCulloch, 2010; J. Hill, Linero, & Murray, 2020). More details can be found in Appendix E of the supplementary materials.

The oracle treatment weight model was the model whose conditional distribution,  $T \mid \mathbf{X}$ , was correctly specified and estimated via ordinary least squares regression. The conditional mean was estimated via ordinary least squares regression, and quantiles were formed assuming Normality. The estimated weight model used the *flexmix* R package to estimate the conditional density of  $T \mid \mathbf{X}$  with a Gaussian mixture distribution with up to 2 mixtures, with the number of mixtures selected via BIC (Gruen & Leisch, 2025).

The conditional mean was assumed linear in the covariates for each mixture component. The BART model with no adjustment used the estimated conditional quantiles without a conformal adjustment.

In all models, the treatment assignment model,  $T \sim N(1, 0.5)$ , was correctly specified for use in the numerator of the weights.

Table 1: Simulation Result: Scenario 1

Situation	Coverage	Length
Oracle model & oracle weights	0.901 (0.003)	9.902 (0.025)
BART outcome model & oracle weights	0.898 (0.003)	13.187 (0.073)
Oracle outcome model & estimated weights	0.902 (0.003)	9.915 (0.024)
BART outcome model & estimated weights	0.895 (0.003)	13.027 (0.064)
BART outcome model & no adjustment	0.717 (0.005)	8.800 (0.056)

Table 2: Simulation Result: Scenario 2

Situation	Coverage	Length
Oracle model & oracle weights	0.901 (0.003)	9.902 (0.025)
BART outcome model & oracle weights	0.900 (0.003)	11.068 (0.034)
Oracle outcome model & estimated weights	0.902 (0.003)	9.915 (0.024)
BART outcome model & estimated weights	0.900 (0.003)	11.080 (0.034)
BART outcome model & no adjustment	0.499 (0.005)	4.643 (0.022)

It is clear from both scenarios that an unadjusted conditional quantile model is not a reasonable model to use. From the other four setups, we can see that the length of the prediction interval depends on the conditional quantile model used. While the method is asymptotically doubly robust, sharp prediction intervals (and hence bands) with nominal

finite sample coverage require a well specified outcome regression model that carefully takes the structure of the response and treatment relationship given the confounders into account. This can be seen by looking at the distribution of the prediction interval lengths in Figure 2, where the prediction bands formed using the oracle outcome regression model are smaller and less variable than those produced using the BART outcome regression model.

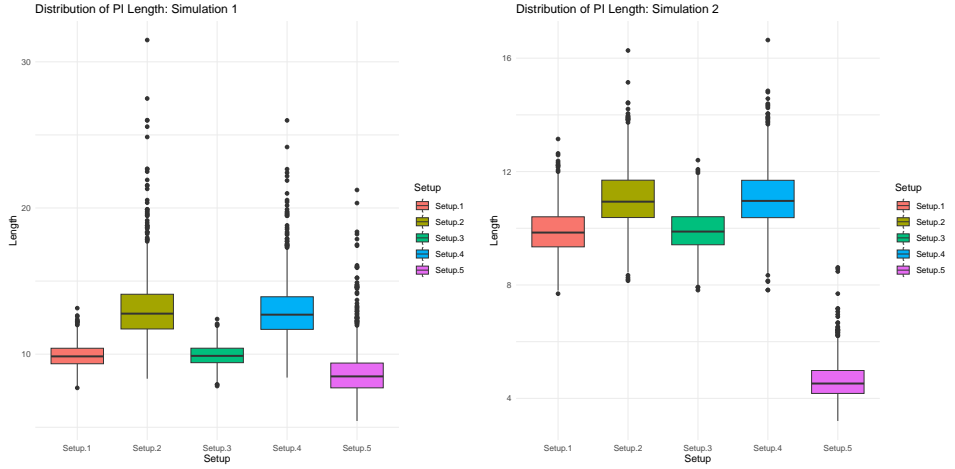


Figure 2: The image on the left is the distribution of the prediction interval lengths from the first simulation. The right image is the distribution of the prediction interval lengths in the second simulation.

### 3.1.1 Treatment Truncation

The motivation for this numerical experiment was given in Section 2. Two scenarios were looked at, one with a homoskedastic error and one with a heteroskedastic error. One covariate,  $X$ , was generated from a standard Normal distribution. The treatment given the covariate,  $T | X$ , was generated from a truncated Normal distribution with a mean of  $X^2 + 1$ . In the homoskedastic case, the variance was one. In the heteroskedastic case, the variance was  $X^2$ . In both scenarios, it was truncated to only take values between 0.5 and 5. The conditional response,  $Y | X, T$  was generated from a Normal distribution with a mean of  $3X + T + X \times T$ . The sample size for each simulation was  $n = 10,000$ . This

was split equally between a training set and a calibration set. Quantile regression and the quantile score function were used. The conditional quantiles were correctly specified and estimated from the data. The simulation number was  $N = 1,000$ . In each simulation, ten additional points were generated. The covariate,  $X$ , and the conditional response,  $Y | T, X$ , were generated in the same way. The treatment was generated from a truncated Normal distribution with a mean of 2 and a variance of 0.8 for both scenarios. It was truncated to take values between 1 and 5. The oracle weights were used and the denominator of the weights was given a slight offset of 0.001. The offset was needed because positivity is not guaranteed in each simulation, so 0.001 is added to the GPS to avoid extremely large weights, and infinite prediction intervals. In practice, positivity is checked for, so no offset is required.

Table 3: Simulation Result: Truncated Treatment

Scenario	Coverage	Length
Homoskedastic	0.950 (0.002)	11.788 (0.186)
Heteroskedastic	0.949 (0.003)	11.796 (0.187)

Here, as with the previous simulation studies, the method works especially well when both the outcome model and the weight model are correctly specified.

## 3.2 Real Data Analysis

The data comes from the 1987 National Medical Expenditure Survey (NMES). It was originally extracted and analyzed by Johnson, Dominici, Griswold, and L. Zeger, 2003, and can now be found in the R package *causalrdf* (Schafer, 2022). Our analysis includes the following subject-level covariates: age at the times of the survey (19–94), age when the individual started smoking, gender (male, female), race (white, black, other), marriage status (married, widowed, divorced, separated, never married), education level (college

graduate, some college, high school graduate, other), census region (Northeast, Midwest, South, West), poverty status (poor, near poor, low income, middle income, high income), and seat belt usage (rarely, sometimes, always/almost always). The response of interest was total medical expenditure (measure in 1987 US dollars). The treatment of interest was *packyear*. It combines self-reported information about frequency and duration of smoking (Johnson, Dominici, Griswold, & L. Zeger, 2003).

$$\text{packyear} = \frac{\text{number of cigarettes per day}}{20} \times \text{number of years smoked}$$

Following Imai and van Dyk, 2004, we use  $\log(\text{packyear})$  as the treatment variable. This allowed us to comfortably use a Normal distribution to estimate the GPS.

Covariate balance or overlap was checked with the method proposed in Flores, Flores-Lagunes, Gonzalez, and Neumann, 2012 and implemented in the R package *causaldrf* (Schafer, 2022). To achieve positivity, 1944 of the 9708 observations were removed. This left us with 7764 observations, which were split evenly into a calibration set and a training set. Selected plots of the covariate distributions can be found in Appendix A of the supplementary materials.

We first computed a population average dose-response curve along with a bootstrapped 95% confidence interval. This can be found in Figure 3. The confidence interval is shaded in gray, while the curve is given by the dashed line. There are 250 randomly selected individuals whose log *packyear* are plotted vs their total medical expenditure as points. From this we can see that the individual variability is not captured by a population average dose-response curve and corresponding confidence interval, as expected. We used the method from Hirano and Imbens, 2004 that is described in Appendix D of the supplementary materials to compute the average dose-response curve.

Next, we randomly selected 5 individuals who were older than 22 and younger than 45 in 1987 to ask the causal question, what is your 90th percentile total medical expenditure if you stop smoking now vs your 90th percentile total medical expenditure if

you continue smoking at 80% of your current rate? We computed 5 prediction intervals for each individual in 3 year increments, and combined them to form prediction bands in both scenarios. For example, if an individual had a packyear level of 10, had been smoking for 10 years, and was 30 at the time of the study, the first prediction interval computed would assume they are now 33 with a packyear level of 10 (the current packyear) + 1 (the average rate their packyear increases)  $\times 0.80$  (80% of the current rate)  $\times 3$  (three year increments) = 12.40. We then use the natural log of 12.40 as the treatment of interest to form the first prediction interval for this individual. Both the  $\log(\text{packyear})$  and age change for each prediction interval, while all other confounders remain the same. This process is repeated 5 times for each individual before the prediction intervals are combined to form prediction bands.

Those comparisons can be found in Figure 4. The covariates for these five individuals can be found in Tables 4 - 5. All individual prediction models were computed using BART. The data were split equally into a training set for the model, and a calibration set to compute non-conformity scores.

The prediction bands for continued smoking were formed assuming that if the individual continued to smoke, their packyears would increase at 80% of their current smoking rate. This was done to help avoid extreme levels of smoking, which would have caused issues with extrapolation. If that rate lead to them having the highest packyear in the dataset, we truncated their packyear to be equal to the highest observed in the dataset. This was only the case for the second individual's last prediction interval.

To form the treatment assignment distribution, we first broke the levels of  $\log(\text{packyear})$  into deciles. The assignment distribution was then a Normal distribution with a mean equal to the mid-point of the treatment of interest's decile and a standard deviation equal to the standard deviation used to estimate the GPS. The decile approach was used because the packyear variable was self-reported by individuals, so we hypothesize that treatments near

each other (in the same decile) are very similar. Therefore, we introduce this discretization to ensure our results are robust. An approach that uses an even larger weight for individuals in the calibration set with a similar packyear to the treatment of interest is shown in Appendix C of the supplementary materials. This corroborates that discretizing the treatment into deciles is robust to slight changes in the treatment assignment distribution. A density plot of the marginal treatment density, along a plot of the treatment assignment distribution can be found in Figure 5.

Formulaically the weights used on the scores for a treatment of interest  $t$  are,

$$W_i = \frac{\phi(T_i \mid d(t), s^2)}{\phi(T_i \mid \hat{\mu}(\mathbf{X}_i), s^2)},$$

where  $d(t)$  is the mid-point of the decile containing  $t$ ,  $\phi(\cdot \mid a, b)$  denotes the density of a Normal distribution with a mean of  $a$  and a variance of  $b$ ,  $\hat{\mu}(\mathbf{x})$  denotes the estimated mean from the GPS, and  $s^2$  the mean squared error from the GPS model.

For each of the five individuals we look at five levels of the potential treatment (smoking level measured by the log of the packyears). For simplicity we ignore the log scale to explain how the treatment and age vary in our analysis. We can view the individual's treatment of interest (the hypothesized packyear) as a function of their age at the baseline plus the change in their age,

$$t(\text{age}_0 + \delta) = t_0 + r\delta,$$

where  $t_0$  is the baseline packyear,  $r$  is 80% of their current rate of smoking, and  $\delta$  is the number of years since 1987 ( $\delta \in \{3, 6, 9, 12, 15\}$  in our analysis). This also allows us to represent the mid-point of the decile of the treatment of interest,

$$d(t(\text{age}_0 + \delta)),$$

Clearly this allows us to incorporate the changes in packyear and age into both the outcome regression model and the weights for the non-conformity scores.

From the plots in Figure 4, we can see the general pattern is that if an individual continues to smoke, their total medical expenditure will increase. These plots can be used

Table 4: Selected Individual's Covariates

Age (1987)	Age when smoking began	Gender	Race	packyear (1987)
35	21	Female	White	22.5
40	19	Male	White	38.5
42	19	Male	White	11
36	15	Female	White	16.5
39	17	Female	White	34.5

Table 5: Selected Individual's Covariates

Marriage	Education	Census Region	Poverty	Seat Belt
Never Married	High School	West	Middle Income	Rarely
Married	Some College	Midwest	High Income	Always
Never Married	High School	West	High Income	Rarely
Married	Some College	Midwest	Middle Income	Always
Never Married	Some College	Midwest	Middle Income	Always

to show individuals who smoke how much they could save over their lifetime, and that there is still a benefit to be had by quitting smoking. For certain individuals, such as the 5th individual, continuing to smoke may greatly increase their total lifetime medical expenditure. Beyond individuals, these costs are also relevant to insurance companies and governments, which fund programs to help individuals quit smoking or offer lower premiums to those who quit smoking (Curry, Grothaus, McAfee, & Pabiniak, 1998; Fishman, Khan, Thompson, & Curry, 2003; Izumi, Tsuji, Ohkubo, et al., 2001).

The general pattern from these plots is that the total lifetime medical expenditure will increase faster for those who continue to smoke than for those who quit. These differences

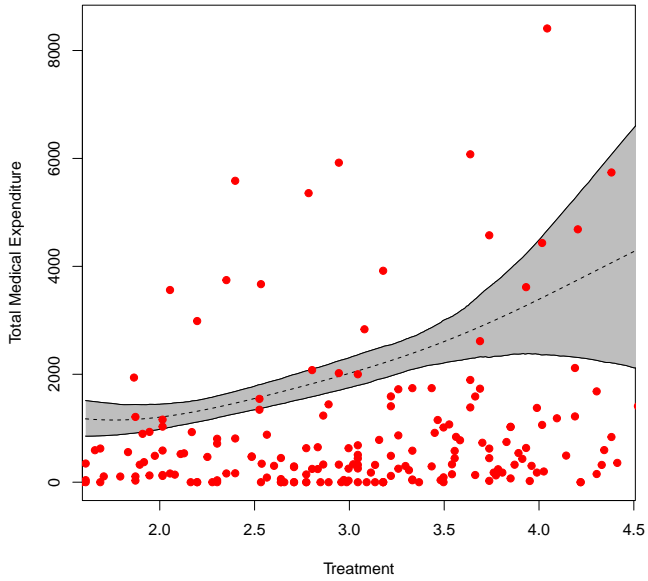


Figure 3: Average dose-response curve and 95% confidence interval. Points are randomly selected participant's observed total medical expenditure.

are likely to be larger for older individuals, similar to those seen for the second and fifth individual. The third individual is a similar age to those two, but has a much lower cumulative smoking load. We would expect to see similarly large differences for the first, third, and fourth individual if we looked further into the future, but we avoid doing so to avoid extreme extrapolation.

## 4 Discussion

From the numerical results, we can see that the individual causal quantile bands have valid prediction coverage when the treatment is randomly assigned according to an assignment distribution, and not according to the observed confounder conditional distribution. They are also easy to visualize, allowing practitioners to easily see the difference between possible treatments, and optimal treatment windows.

IPB adds uncertainty quantification with minimal assumptions to individualized dose-

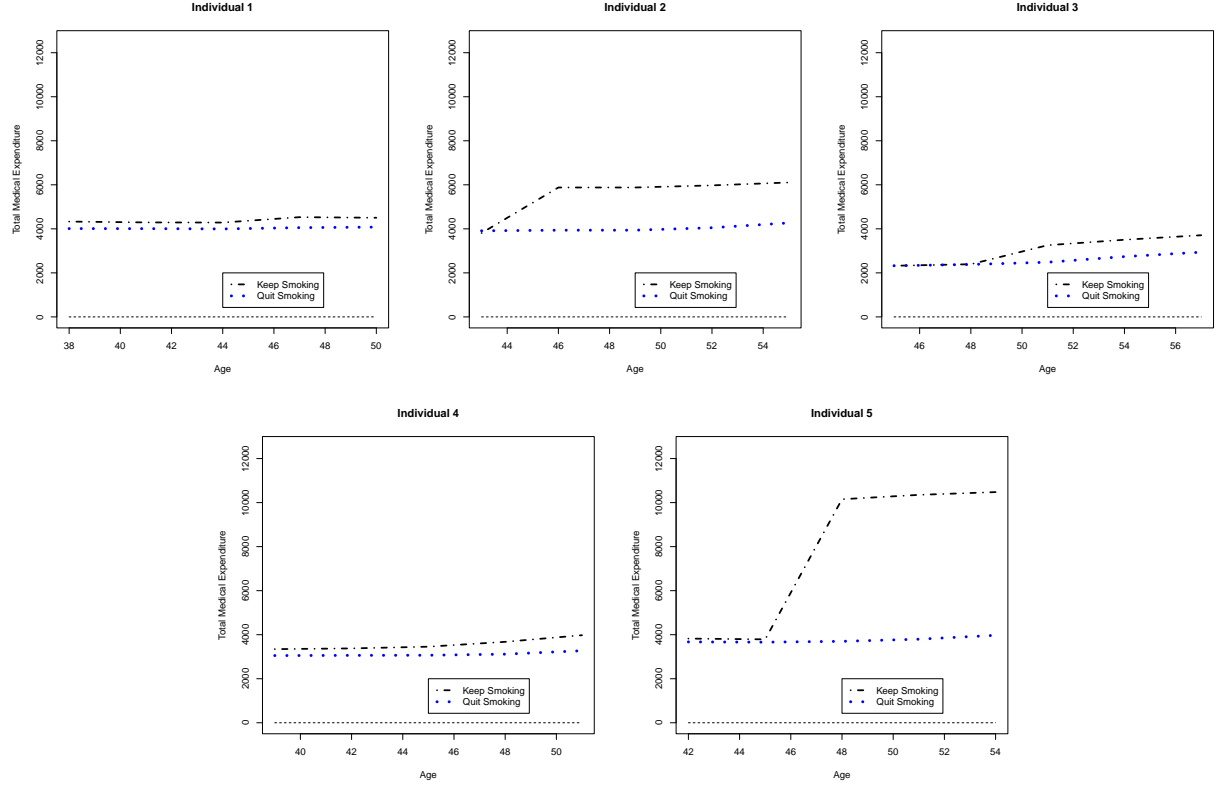
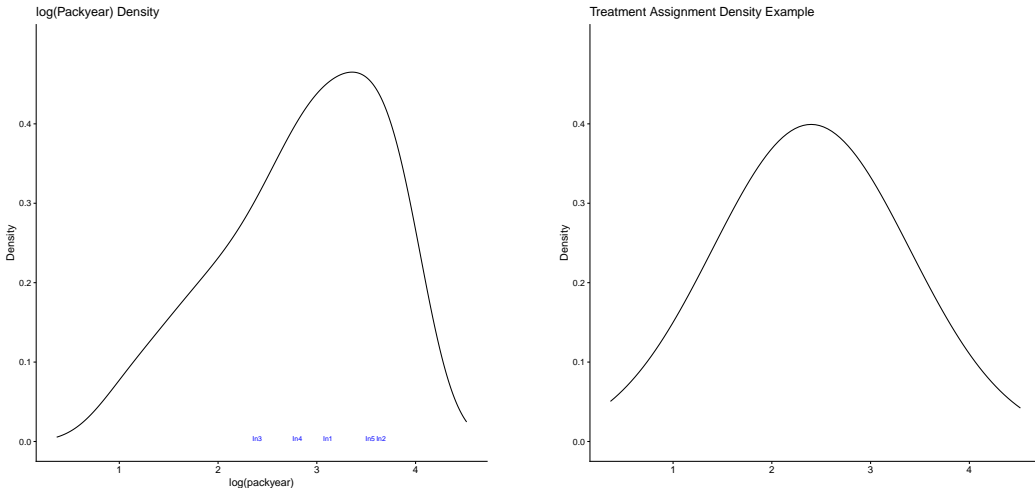


Figure 4: 90% upper conformal prediction intervals for continued smoking are given by the black dashed lines. 90% upper prediction intervals for quitting smoking are given by the blue line.

response curves. This method is unique compared to the existing methods because it starts with a quantile estimate, instead of a conditional mean estimate, allowing our method to enjoy doubly robust coverage properties. The method is also flexible enough to allow practitioners to see what would happen if they assigned treatments in a targeted way, and not only uniformly. Further work can be done exploring conditional treatment assignment models, instead of the unconditional treatment assignment models that we focused on.



(a) A marginal density plot of the  $\log(\text{packyear})$  variable, along with the selected individual's packyear value plotted.

(b) The treatment assignment density with a decile midpoint equal to the starting level for the third individual.

Figure 5: Treatment Distributions (on the same scales)

## 5 References

Chipman, H. A., George, E. I., & McCulloch, R. E. (1998). Bayesian cart model search. *Journal of the American Statistical Association*, 93(443), 935–948.

Chipman, H. A., George, E. I., & McCulloch, R. E. (2010). Bart: Bayesian additive regression trees. *Ann. Appl. Stat.*, 4(1), 266–298. <https://doi.org/10.1214/09-AOAS285>

Curry, S. J., Grothaus, L. C., McAfee, T., & Pabiniak, C. (1998). Use and cost effectiveness of smoking-cessation services under four insurance plans in a health maintenance organization. *New England Journal of Medicine*, 339(10), 673–679.

Dorie, V., Chipman, H., & McCulloch, R. (2025). *Dbarts: Discrete bayesian additive regression trees sampler* [R package version 0.9-32]. <https://doi.org/10.32614/CRAN>. package.dbarts

Fishman, P. A., Khan, Z. M., Thompson, E. E., & Curry, S. J. (2003). Health care costs among smokers, former smokers, and never smokers in an hmo. *Health services research, 38*(2), 733–749.

Flores, C. A., Flores-Lagunes, A., Gonzalez, A., & Neumann, T. C. (2012). Estimating the effects of length of exposure to instruction in a training program: The case of job corps. *The Review of Economics and Statistics, 94*(1), 153–171. Retrieved February 27, 2023, from <http://www.jstor.org/stable/41349166>

Fort, M. (2016). Unconditional and conditional quantile treatment effect: Identification strategies and interpretations. In G. Alleva & A. Giommi (Eds.), *Topics in theoretical and applied statistics* (pp. 15–24). Springer International Publishing.

Gruen, B., & Leisch, F. (2025). *Flexmix: Flexible mixture modeling* [R package version 2.3-20]. <https://doi.org/10.32614/CRAN.package.flexmix>

Hernán, M., & Robins, J. (2020). *Causal inference: What if*. Boca Raton: Chapman & Hall/CRC.

Hill, J., Linero, A., & Murray, J. (2020). Bayesian additive regression trees: A review and look forward. *Annual Review of Statistics and Its Application, 7*(1), 251–278.

Hill, J. L. (2011). Bayesian nonparametric modeling for causal inference. *Journal of Computational and Graphical Statistics, 20*(1), 217–240.

Hirano, K., & Imbens, G. W. (2004). The propensity score with continuous treatments. In *Applied bayesian modeling and causal inference from incomplete-data perspectives* (pp. 73–84). John Wiley & Sons, Ltd. <https://doi.org/10.1002/0470090456.ch7>

Imai, K., & Ratkovic, M. (2015). Robust estimation of inverse probability weights for marginal structural models. *Journal of the American Statistical Association, 110*(511), 1013–1023.

Imai, K., & van Dyk, D. A. (2004). Causal inference with general treatment regimes. *Journal*

*of the American Statistical Association*, 99(467), 854–866. <https://doi.org/10.1198/016214504000001187>

Imbens, G. (2000). The role of the propensity score in estimating dose-response functions.

*Biometrika*, 87(3), 706–710.

Imbens, G. W., & Wooldridge, J. M. (2009). Recent developments in the econometrics of

program evaluation. *Journal of Economic Literature*, 47(1), 5–86. <https://doi.org/10.1257/jel.47.1.5>

Izumi, Y., Tsuji, I., Ohkubo, T., Kuwahara, A., Nishino, Y., & Hisamichi, S. (2001). Impact

of smoking habit on medical care use and its costs: A prospective observation of na-

tional health insurance beneficiaries in japan. *International Journal of Epidemiology*,

30(3), 616–621.

Johnson, E., Dominici, F., Griswold, M., & L. Zeger, S. (2003). Disease cases and their

medical costs attributable to smoking: An analysis of the national medical expendi-

ture survey. *Journal of Econometrics*, 112(1), 135–151. <https://EconPapers.repec.org/RePEc:eee:econom:v:112:y:2003:i:1:p:135-151>

Koenker, R., & Bassett, G. (1978). Regression quantiles. *Econometrica*, 46(1), 33–50. Re-

trieved March 19, 2023, from <http://www.jstor.org/stable/1913643>

Lechner, M. (2001). Identification and estimation of causal effects of multiple treatments

under the conditional independence assumption. In M. Lechner & F. Pfeiffer (Eds.),

*Econometric evaluation of labour market policies* (pp. 43–58). Physica-Verlag HD.

Lei, J., G'Sell, M., Rinaldo, A., Tibshirani, R. J., & Wasserman, L. (2018). Distribution-free

predictive inference for regression. *Journal of the American Statistical Association*,

113(523), 1094–1111. <https://doi.org/10.1080/01621459.2017.1307116>

Lei, L., & Candès, E. J. (2021). Conformal Inference of Counterfactuals and Individual Treatment Effects. *Journal of the Royal Statistical Society Series B: Statistical Methodology*, 83(5), 911–938. <https://doi.org/10.1111/rssb.12445>

Linusson, H., Johansson, U., & Löfström, T. (2014). Signed-error conformal regression. *Advances in Knowledge Discovery and Data Mining*, 224–236.

Neyman, J. (1923). On the application of probability theory to agricultural experiments. essay on principles. section 9. *Statistical Science*, 5(4), 465–472. Retrieved March 17, 2023, from <http://www.jstor.org/stable/2245382>

Papadopoulos, H., Proedrou, K., Vovk, V., & Gammerman, A. (2002). Inductive confidence machines for regression. *Machine Learning: ECML 2002*, 345–356.

R Core Team. (2023). *R: A language and environment for statistical computing*. R Foundation for Statistical Computing. Vienna, Austria. <https://www.R-project.org/>

Robins, J., Hernán, M., & Brumback, B. (2000). Marginal structural models and causal inference in epidemiology. *Epidemiology (Cambridge, Mass.)*, 11(5), 550–560. <https://doi.org/10.1097/00001648-200009000-00011>

Romano, Y., Patterson, E., & Candes, E. (2019). Conformalized quantile regression. *Advances in Neural Information Processing Systems*, 32. [https://proceedings.neurips.cc/paper\\_files/paper/2019/file/5103c3584b063c431bd1268e9b5e76fb-Paper.pdf](https://proceedings.neurips.cc/paper_files/paper/2019/file/5103c3584b063c431bd1268e9b5e76fb-Paper.pdf)

Rosenbaum, P. R., & Rubin, D. B. (1983). The central role of the propensity score in observational studies for causal effects. *Biometrika*, 70(1), 41–55. Retrieved March 17, 2023, from <http://www.jstor.org/stable/2335942>

Rosenbaum, P. R., & Rubin, D. B. (1984). Reducing bias in observational studies using subclassification on the propensity score. *Journal of the American Statistical Association*, 79(387), 516–524. Retrieved March 17, 2023, from <http://www.jstor.org/stable/2288398>

Rubin, D. B. (1978). Bayesian Inference for Causal Effects: The Role of Randomization. *The Annals of Statistics*, 6(1), 34–58. <https://doi.org/10.1214/aos/1176344064>

Schafer, J. (2022). *Causaldrf: Estimating causal dose response functions* [R package version 0.4.2]. <https://CRAN.R-project.org/package=causaldrf>

Schröder, M., Frauen, D., Schweisthal, J., Heß, K., Melnychuk, V., & Feuerriegel, S. (2025). Conformal prediction for causal effects of continuous treatments. <https://arxiv.org/abs/2407.03094>

Schwab, P., Linhardt, L., Bauer, S., Buhmann, J. M., & Karlen, W. (2020). Learning counterfactual representations for estimating individual dose-response curves. *Proceedings of the AAAI Conference on Artificial Intelligence*, 34(04), 5612–5619. <https://doi.org/10.1609/aaai.v34i04.6014>

Shalit, U., Johansson, F. D., & Sontag, D. A. (2016). Estimating individual treatment effect: Generalization bounds and algorithms. *International Conference on Machine Learning*. <https://api.semanticscholar.org/CorpusID:320456>

Shen, X., Liu, T., Xu, S., Chen, B., Tang, X., Xiao, J., & Qin, Y. (2022). Optimal Timing of Anterior Cruciate Ligament Reconstruction in Patients With Anterior Cruciate Ligament Tear: A Systematic Review and Meta-analysis. *JAMA Network Open*, 5(11), e2242742–e2242742. <https://doi.org/10.1001/jamanetworkopen.2022.42742>

Shimodaira, H. (2000). Improving predictive inference under covariate shift by weighting the log-likelihood function. *Journal of Statistical Planning and Inference*, 90(2), 227–244. [https://doi.org/https://doi.org/10.1016/S0378-3758\(00\)00115-4](https://doi.org/https://doi.org/10.1016/S0378-3758(00)00115-4)

Tibshirani, R. J., Foygel Barber, R., Candes, E., & Ramdas, A. (2019). Conformal prediction under covariate shift. *Advances in Neural Information Processing Systems*, 32. [https://proceedings.neurips.cc/paper\\_files/paper/2019/file/8fb21ee7a2207526da55a679f0332de2-Paper.pdf](https://proceedings.neurips.cc/paper_files/paper/2019/file/8fb21ee7a2207526da55a679f0332de2-Paper.pdf)

Tu, C. (2019). Comparison of various machine learning algorithms for estimating generalized propensity score. *Journal of Statistical Computation and Simulation*, 89(4), 708–719.

Verhaeghe, J., Jonkers, J., & Van Hoecke, S. (2024). Conformal prediction for dose-response models with continuous treatments. *arXiv preprint arXiv:2409.20412*.

Vovk, V., Gammerman, A., & Shafer, G. (2005). *Algorithmic learning in a random world*. Springer-Verlag.

Westreich, D., & Cole, S. R. (2010). Invited Commentary: Positivity in Practice. *American Journal of Epidemiology*, 171(6), 674–677. <https://doi.org/10.1093/aje/kwp436>

Zhang, Z., Chen, Z., Troendle, J. F., & Zhang, J. (2012). Causal inference on quantiles with an obstetric application. *Biometrics*, 68(3), 697–706. Retrieved April 13, 2023, from <http://www.jstor.org/stable/23270587>

Zhao, S., van Dyk, D., & Imai, K. (2020). Propensity score-based methods for causal inference in observational studies with non-binary treatments. *Statistical Methods in Medical Research*, 29, 709–727. <https://doi.org/10.1177/0962280219888745>

## Appendix of IPB

The appendix of IPB contains 5 sections. The first contains distributional plots of some of the variables used in the real data analysis. The second is a comparison of IPB vs a uniform treatment assignment. The third conducts the real data analysis with a different treatment assignment distribution that more heavily weights individuals in the calibration set who have a treatment in the same decile as the treatment of interest. The fourth reviews the generalized propensity score. The final section is a discussion of BART and its priors.

## A Real Data Plots

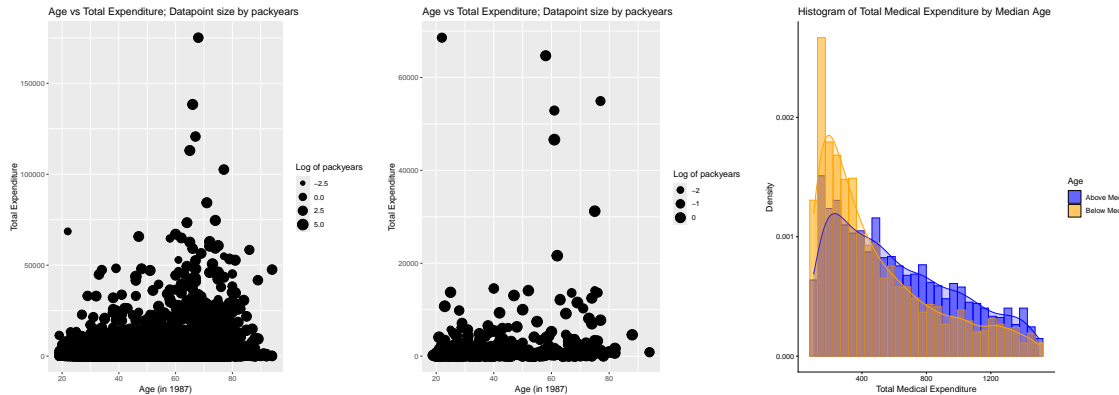


Figure 6: The first plot is the full data, the second is a subsample. These plots don't appear to provide very much information because there is a point mass at \$0 for expenditure. The last plot is the distribution of total medical expenditure for those older than 48 and younger than 48. Total medical expenditure was truncated to be between the first and third quartile (\$100 and \$1500) because of the large point mass at zero, as well as extreme outliers.

## B Uniform Assignment Assumed

We look at a similar simulation setup to the one used in the second scenario in Section 3.1 of the main text, with the differences being that the treatment assignment distribution

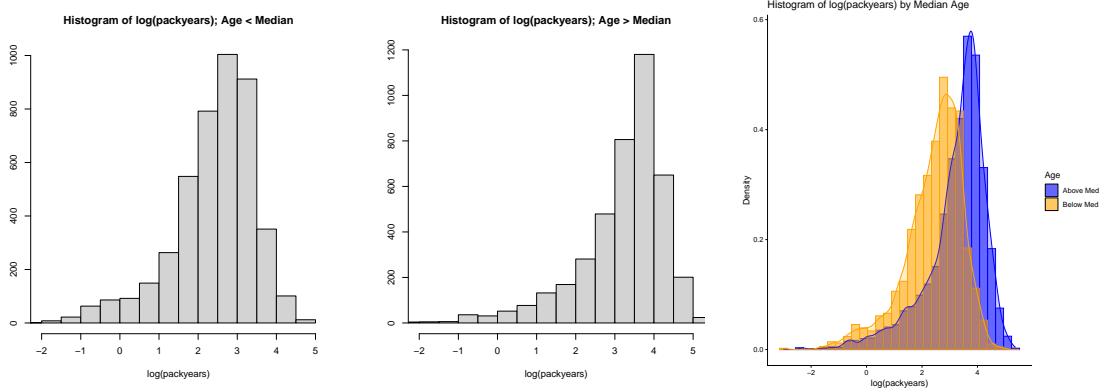


Figure 7: The first plot is a histogram of the treatment for those younger than 48 (the median age) in 1987. The second plot is the same histogram, but for those older than 48. The combined plot is the third plot.

was  $N(1, 4)$ , instead of  $N(1, 8.25)$ , and 200 out of sample data points were used for each simulation instead of 10. We compare the weights used with IPB, with those suggested by Verhaeghe, Jonkers, and Van Hoecke, 2024, replacing the treatment assignment distribution in the numerator of the weights with a uniform distribution. Both approaches use the oracle conditional mean, with the absolute difference non-conformity score,  $|\mu(\mathbf{X}, T) - Y|$ . The target coverage level was 90%. The coverage results can be found in Table 6. A comparison of the distribution of the lengths can be found in Figure 8.

Table 6: Simulation Result: IPB vs Uniform Treatment Assignments

Situation	Coverage	Length
IPB	0.887 (0.001)	20.966 (0.165)
Uniform Weights	0.892 (0.001)	21.747 (0.231)

From this simulation it is easy to see that the coverage is fairly robust when the treatment assignment distribution is not correctly specified. When looking at the distribution of prediction interval lengths, we can see that using a uniform distribution instead of the treatment assignment leads to a larger variability, which is similar to ignoring the marginal

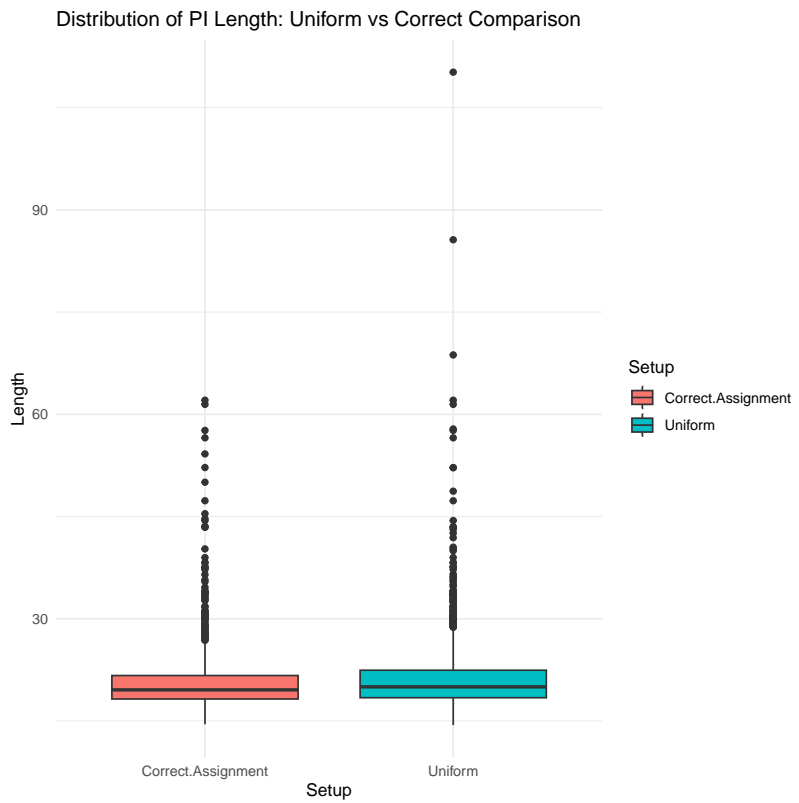


Figure 8: The boxplots represent the distribution of the prediction interval lengths for both methods.

treatment distribution when using the GPS as the denominator in a marginal structural model (Robins, Hernán, & Brumback, 2000).

## C Real Data Analysis Differing Deciles

We conducted the real data analysis twice more, showing that if a practitioner wanted to put more weight on treatments in one decile without using a truncated treatment, they are able to.

If the treatment of interest and the observed treatment of an individual in the calibration set were in the same decile, the assignment was a Normal distribution with a mean equal to the mid-point of the treatment of interest's decile and a standard deviation equal to the standard deviation used to estimate the GPS. If the treatment of interest and the observed

treatment of an individual in the calibration set were in different deciles, the assigned weight was  $k$  the weight that would have been used if the observations were in the same decile, where  $k$  is a practitioner selected parameter. This allowed us to use an approach similar to a kernel density, but with a larger weight for individuals in the calibration set with a similar packyear to the treatment of interest. Formulaically the weights used on the scores for a treatment of interest  $t$  are,

$$W_i = \begin{cases} \frac{\phi(T_i|d,s^2)}{\phi(T_i|\hat{\mu}(\mathbf{X}_i),s^2)}, & \text{if } T_i \text{ is in the same decile as } t, \\ k \times \frac{\phi(T_i|d,s^2)}{\phi(T_i|\hat{\mu}(\mathbf{X}_i),s^2)}, & \text{if } T_i \text{ is in a different decile than } t, \end{cases}$$

where  $d$  is the mid-point of the decile containing  $t$ ,  $\phi(\cdot | a, b)$  denotes the density of a Normal distribution with a mean of  $a$  and a variance of  $b$ ,  $\hat{\mu}(\mathbf{x})$  denotes the estimated mean from the GPS,  $s^2$  the mean squared error from the GPS model, and  $k$  the weight for observations in the calibration set with a treatment outside of the same decile. The plots from the analysis redone with  $k = 1/2$  can be found in Figure 9 and for  $k = 1/4$  in Figure 10.

We can see from the plots that adjusting  $k$  does not change the results at all. Due to the weighted quantile, the final selected quantile is the same for  $k = 1$ ,  $1/2$ , and  $1/4$ . This provides confidence that the patterns that emerge from using IPB are robust when the treatment allocation distributions are similar.

## D Generalized Propensity Score

The generalized propensity score was introduced by Hirano and Imbens, 2004, though the idea existed before then, see Robins, Hernán, and Brumback, 2000 for one example. It is defined as the conditional density of  $T$  given  $\mathbf{X}$ ,  $r(t, \mathbf{x}) = f(T = t | \mathbf{X} = \mathbf{x})$ . A further generalization of the generalized propensity score is the propensity function (PF).

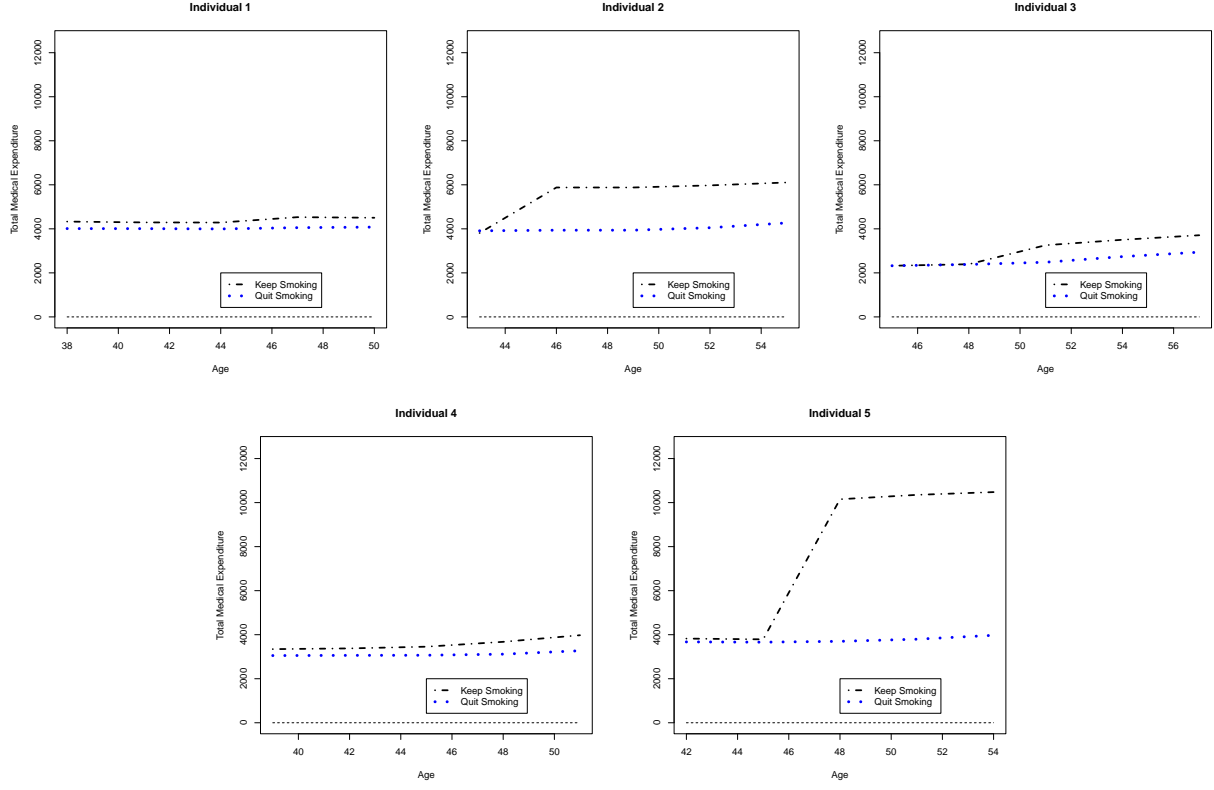


Figure 9: 90% upper conformal prediction intervals for continued smoking are given by the black dashed lines. 90% upper prediction intervals for quitting smoking are given by the blue line. The treatment assignment distribution used a ratio of  $k = 1/2$ .

Proposed by Imai and van Dyk, 2004, they assume the conditional density of  $T$  given  $\mathbf{X}$  is indexed by  $\psi$ . That is,  $f(\cdot | \mathbf{X}) = f_\psi(\cdot | \mathbf{X})$ . If the density only depends on  $\mathbf{X}$  through a finite dimensional quantity  $\theta_\psi(\mathbf{X})$ , then the propensity function can be rewritten as  $f(\cdot | \theta_\psi(\mathbf{X}))$ .

Imai and van Dyk, 2004 showed that, under strong ignorability, the PF has two useful properties. First, it is a balancing score, meaning that conditional on the PF, the treatment assignment is independent of the covariates. Second, given the PF, the treatment assignment and the potential outcomes are independent. Another way of phrasing that is, given the PF the treatment assignment is strongly ignorable,  $(T \perp\!\!\!\perp \mathcal{Y} | \theta_\psi(\mathbf{X}))$ . Practically, this means that high dimensional covariates that satisfy strong ignorability can be represented

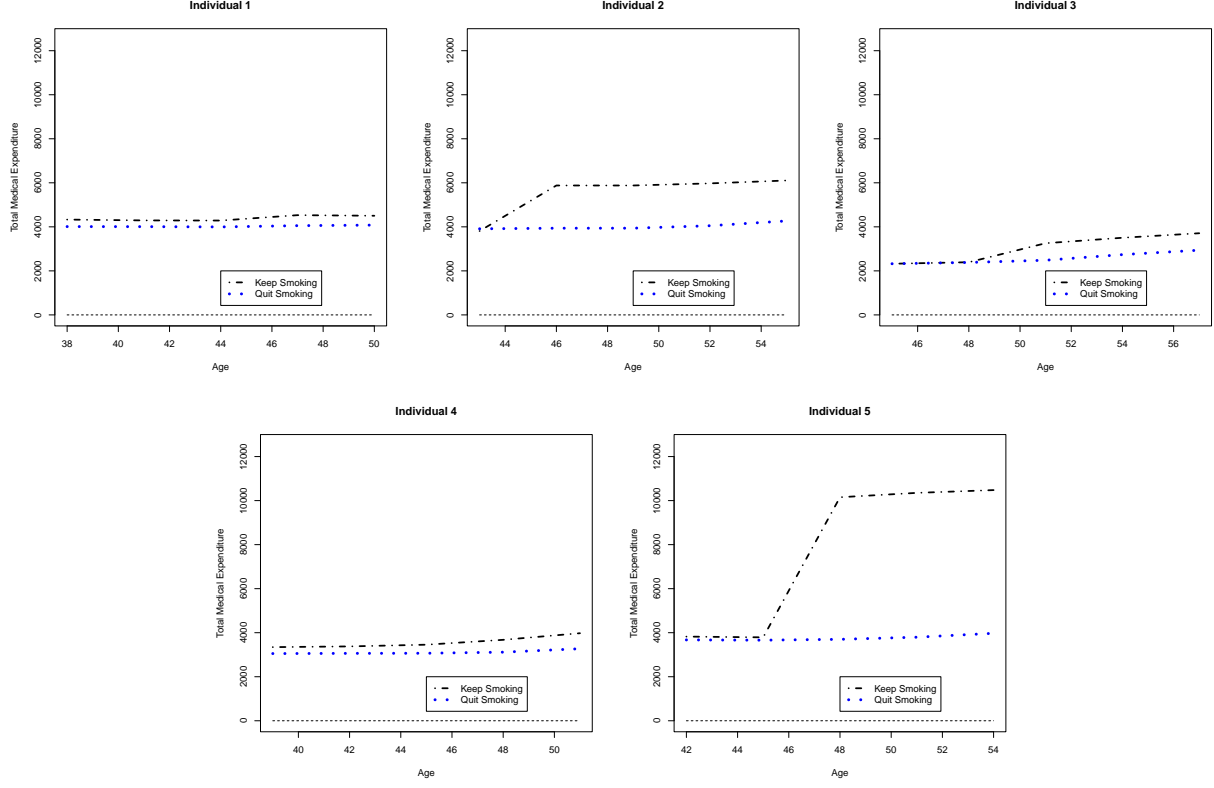


Figure 10: 90% upper conformal prediction intervals for continued smoking are given by the black dashed lines. 90% upper prediction intervals for quitting smoking are given by the blue line. The last plot is a density plot of the packyear variable, along with the selected individual's packyear value plotted. The treatment assignment distribution used a ratio of  $k = 1/4$ .

in a lower dimension without introducing bias. The PF still needs to be estimated using the data. It can be written as  $\theta(\mathbf{X}_i, \hat{\psi}) = \hat{\theta}_i$ , or  $\hat{\theta}_i$  in the scalar case.

Robins, Hernán, and Brumback, 2000 introduced the idea of a marginal structural models. These are an extension of inverse probability treatment weighting to the continuous treatment setting with an assumed parametric form of the dose-response curve. For example, if the function is linear,  $\mu(t) = \beta_0 + \beta_1 t$ , the method estimates  $\beta_0$  and  $\beta_1$  by a least-squares calculation that minimizes

$$\sum_i^N w_i(T_i)(Y_i - \beta_0 - \beta_1 T_i)^2,$$

where  $w_i(T_i)$  is a weight. A squared treatment term could also be included to be more robust. Both of these are examples of marginal structural models. A common weight is the inverse of the generalized propensity score,  $w_i(T_i) = \frac{1}{f(T_i|\mathbf{X}_i)}$ .

As in the binary case, these weights can be unstable or highly variable for observed treatment values that fall in the tails. Robins, Hernán, and Brumback, 2000 recommend using stabilized weights  $w_i(T) = \frac{f(T_i)}{f(T_i|\mathbf{X}_i)}$ , where  $f(T_i)$  is the marginal density of the treatment. This is similar to the idea of importance sampling. What might have occurred if the treatment was assigned at random instead of having been assigned according to the conditional density. That is, if it had been assigned according to  $f(T_i)$  instead of  $f(T_i | \mathbf{X}_i)$ .

Imai and van Dyk, 2004 recommended subclassifying the data based on the PF, and estimating causal effects within each subclass. Assuming that the PF is correctly specified, within subclasses the covariates are evenly distributed across treatment levels. Then, within subclasses, the outcome can be modeled as a function of the treatment. For example, in each subclass model the response as  $Y = \beta_0 + \beta_1 T + \beta_2 T^2 + \epsilon$ . Then final estimates can be computed by weighting how many observations were in each subclass. For example, the average treatment effect at  $T = t$  could be computed by  $\hat{\mu}(t) = \sum_j^g \frac{n_j}{n} \hat{f}_j(t)$ , where  $g$  is the number of subclass or groups,  $n_j$  is the number of individuals in each subclass,  $n$  is the total sample size, and  $\hat{f}_i$  is the estimated response in the  $i$ -th subclass.

Hirano and Imbens, 2004 proposed using the GPS as an “imputation” tool. Their method consists of three steps. The first is to fit a parametric model to the treatment given the covariates. They specifically used the normal distribution for their conditional distribution,  $T | X \sim \mathcal{N}(\mathbf{X}^T \beta, \sigma^2)$

$$\hat{R}_i = \frac{1}{\sqrt{2\pi\hat{\sigma}^2}} \exp\left(-\frac{1}{2\hat{\sigma}^2}(T_i - \mathbf{X}_i^T \hat{\beta})^2\right).$$

The second step is to model the conditional expectation of  $Y$  given  $T$  and  $\hat{R}$ . They used a quadratic approximation,

$$E(Y_i | T_i, \hat{R}_i) = \alpha_0 + \alpha_1 T_i + \alpha_2 T_i^2 + \alpha_3 \hat{R}_i + \alpha_4 \hat{R}_i^2 + \alpha_5 T_i \hat{R}_i,$$

where the parameters,  $\alpha_i$  are to be estimated. One common method is ordinary least squares. The final step is to estimate the average dose-response function at a particular treatment value,  $t$ .

$$\hat{\mu}(t) = \frac{1}{n} \sum_{i=1}^n (\hat{\alpha}_0 + \hat{\alpha}_1 t + \hat{\alpha}_2 t^2 + \hat{\alpha}_3 \hat{r}(t, \mathbf{X}_i) + \hat{\alpha}_4 \hat{r}(t, \mathbf{X}_i)^2 + \hat{\alpha}_5 t \hat{r}(t, \mathbf{X}_i))$$

This idea was extended by Zhao, van Dyk, and Imai, 2020, but they used a smooth coefficient model that can vary as a function of the propensity score instead of a fixed parameter in each subclass. That is, they modeled the conditional response as  $E(Y | T, \hat{\theta}) = f(\hat{\theta}) + g(\hat{\theta})T$ , where  $h(\cdot)$  and  $g(\cdot)$  are assumed to be smooth and  $\hat{\theta}$  is the estimated PF.

The first step is to model the treatment given the covariates, and estimate a PF for each subject,  $\hat{\theta}_i$ . The next step is to fit a smooth coefficient model for the response given the treatment and the estimated PF,  $E(Y | \hat{\theta}, T) = f(\hat{\theta}, T)$ . This gives us an estimated function,  $\hat{f}(\hat{\theta}_i, T_i)$ . The final step is to average over the  $n$  estimated PF values we have to get an estimated average dose-response function at a particular treatment value of interest,  $t$ .  $\hat{\mu}(t) = \frac{1}{n} \sum_{i=1}^n \hat{f}(\hat{\theta}_i, t)$ . The smooth coefficient model in the second step can be a flexible model, such as a generalized additive model (GAM).

Flores, Flores-Lagunes, Gonzalez, and Neumann, 2012 extended the method of Hirano and Imbens, 2004 by modeling the conditional expectation of  $Y$  given  $T$  and  $\hat{R}$  non-parametrically. They then compute the estimated average dose-response at a given value of the treatment in the same way as Hirano and Imbens, 2004 and Zhao, van Dyk, and Imai, 2020.

Flores, Flores-Lagunes, Gonzalez, and Neumann, 2012 also proposed a second method that involves applying a Horvitz-Thompson weighting scheme to a continuous treatment. This can also be thought of as a generalized propensity score version of inverse probability weighting.

To give the idea, assume that that a generalized propensity score has already been

calculated,  $\hat{R}_i$ . First, bin the treatments. Then, let the number of bins increase while length of bins goes to zero. This mimics what happens when a treatment is truly continuous. Weight each response by 1 over the estimated GPS. That gives an estimate of the average dose-response at a specific value of  $t$ ,

$$\hat{\mu}(t) = \frac{1}{n} \frac{\sum_i^n \mathbb{1}(T_i \in \Delta) Y_i}{2h\hat{R}_i},$$

where  $h$  is a sequence of numbers going to 0 as  $n \rightarrow \infty$  and  $\Delta = [t - h, t + h]$ . Note also that  $P(T_i \in \Delta) \approx 2h\hat{R}_i$  for small values of  $h$ .

This can be smoothed out by using a kernel function.

$$\hat{\mu}(t) = \frac{\sum_i^n K_h(T_i - t) Y_i w_i(t)}{\sum_i^n K_h(T_i - t) w_i(t)},$$

where  $K_h(\cdot)$  is a kernel function,  $h$  is a bandwidth satisfying  $h \rightarrow 0$  and  $nh \rightarrow \infty$  as  $n \rightarrow \infty$ , and  $w_i(\cdot)$  are the inverse of the generalized propensity score.

Stabilized weights can also be used instead of unstabilized weights. This is recommended by Zhao, van Dyk, and Imai, 2020. Notice that the weights now use the observed treatment instead of the treatment of interest. Let  $\tilde{K}(T_i - t) = \frac{f(T_i)}{f(T_i | \mathbf{X}_i)} K_h(T_i - t)$ . Then our estimated average dose-response function is

$$\hat{\mu}(t) = \frac{\sum_i^n \tilde{K}_h(T_i - t) Y_i}{\sum_i^n \tilde{K}_h(T_i - t)},$$

Another approach that Flores, Flores-Lagunes, Gonzalez, and Neumann, 2012 looked at was to use a local linear regression.

$$\hat{\mu}(t) = \frac{D_o(t)S_2(t) - D_1(t)S_1(t)}{S_0(t)S_2(t) - S_1^2(t)},$$

where  $S_j(t) = \sum_i^n \tilde{K}_h(T_i - t)(T_i - t)^j$  and  $D_j(t) = \sum_i^n \tilde{K}_h(T_i - t)(T_i - t)^j Y_i$ .

## E BART

In general BART is designed to estimate models of the form

$$Y = f(\mathbf{x}) + \epsilon, \tag{2}$$

where  $\epsilon \sim N(0, \sigma^2)$ ,  $Y$  is the response, and  $\mathbf{x}$  is the vector of covariates (Chipman, George, & McCulloch, 2010). Because of how important the treatment group notation is in causal inference, it can be helpful to write (2) as

$$Y = f(t, \mathbf{x}) + \epsilon, \quad (3)$$

where  $\epsilon$  in (3) is the same as in (2),  $Y$  is the response,  $t$  is the treatment assignment, and  $\mathbf{x}$  is the vector of pretreatment variables. In the continuous treatment case,  $f(t, \mathbf{x}) = E(Y(t)|\mathbf{X} = \mathbf{x})$ ,  $\forall t \in \mathcal{T}$ .

Let  $T$  denote a binary tree. The tree consists of all its decision rules that lead down to the bottom nodes. Figure 11 shows an example of a single tree with one pretreatment variable and a treatment assignment variable. The decisions send the tree to the left, so if  $Z = 0$  the tree would then check if  $X_1 < 20.7428$  before ending at a node. Each bottom node has a parameter that is associated with it. For the  $j^{th}$  node this parameter is  $\mu_j$ , which is the mean response of the observations that fall into the node. Let  $\mathbf{M}$  denote the vector of mean values for  $b$  nodes,  $\mathbf{M} = \{\mu_1, \dots, \mu_b\}$  where  $b$  is the number of nodes for the tree.

Given a tree model  $(T, \mathbf{M})$  and a pair of treatment assignments and pretreatment variables  $(t, \mathbf{x})$ , define  $g(t, \mathbf{x}; T, \mathbf{M})$  as the value obtained by “dropping”  $(t, \mathbf{x})$  down the tree  $(T, \mathbf{M})$ . For example, using the tree in Figure 11 with  $(z, x) = (1, 50)$ ,  $g(1, 50, T, \mathbf{M}) = 112.40$ . BART allows the user to approximate (3) with

$$Y = g(z, \mathbf{x}; T_1, \mathbf{M}_1) + g(z, x; T_2, \mathbf{M}_2) + \dots + g(z, \mathbf{x}; T_m, \mathbf{M}_m) + \epsilon,$$

where each  $(T_j, \mathbf{M}_j)$  denotes a single subtree model and  $\epsilon$  is as before in (3). The sum-of-trees model works to estimate this by fitting the first tree model,  $g(t, \mathbf{x}, T_1, \mathbf{M}_1)$ . It then finds the residuals of the response and the first tree model, fits a tree to those residuals, and continues to do that a total of  $m$  times. To avoid overfitting, a regularization prior is used on  $(T_j, \mathbf{M}_j)$ . This allows each tree to only contribute a small part to the overall fit

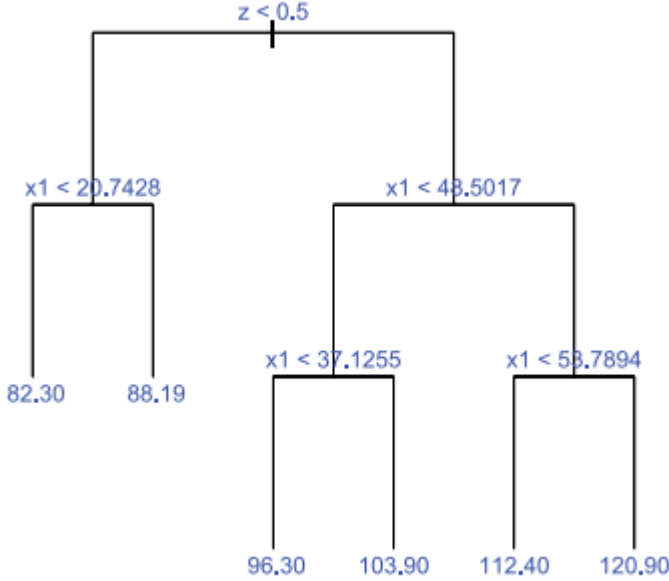


Figure 11: The binary tree fit to example data from J. L. Hill, 2011.

of the model. Each set of  $(T_j, \mathbf{M}_j)$  and  $\sigma$  are treated as parameters in a model, they are given empirical priors, and they are redrawn during each MCMC iteration.

During each MCMC iteration, each tree can shrink, grow, or change nonterminal node rules (Chipman, George, & McCulloch, 2010; J. L. Hill, 2011). For more details on the algorithm and how it works see Chipman, George, and McCulloch, 2010. The default prior has a preference for  $T_j$  that have a small number of terminal nodes and a preference for  $\mu_k$  that are 0 (the response is centered in BART). These combined help prevent the model from overfitting. Of course, if the data suggests large trees, the prior for small trees and a small number of terminal nodes can be overcome. An example of a BART fit is given in Figure 12

It was shown in Chipman, George, and McCulloch, 2010 that the performance of BART is competitive with the default values for the number of trees, the number of MCMC iterations, and the priors compared to model fitting methods that require cross-validation. The default number of trees is 200, the default number of MCMC iterations is 1,000 with a default of 100 iterations for burn-in. This allows BART to be more “automatic” or easier

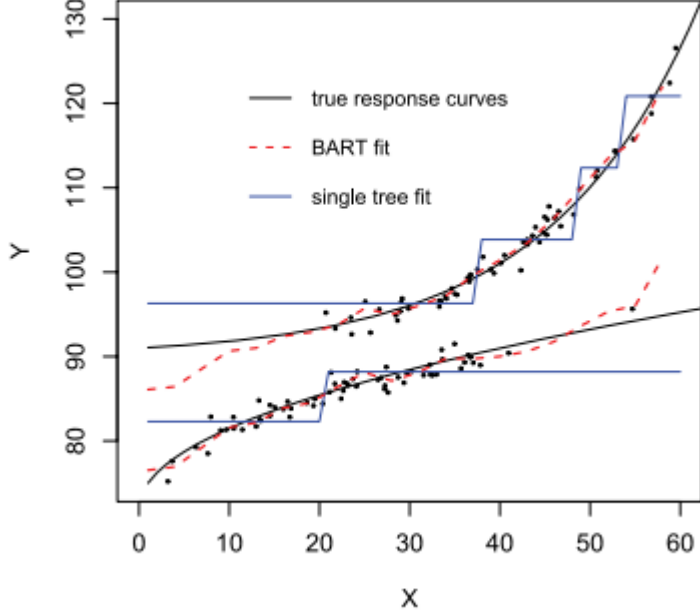


Figure 12: The BART fit using the same data as in Figure 11. The black points are the data, the dashed red line is the BART fit, the solid blue line is the fit with one tree, and the solid black line is the true curve (J. L. Hill, 2011).

to implement and apply compared to other methods. Because it is a sum-of-trees model, BART is able to capture linear terms easily. BART can also capture interaction terms. For example, a parent node could split at a binary treatment,  $x_1$ . Both nodes under that split could then split at another binary variable  $x_2$ . The terminal nodes under the splits at  $x_2$  need not be monotonic, they could change based on the values that both  $x_1$  and  $x_2$  take. Because the tree can become larger or smaller during each iteration, it allows the level of interaction to be closely approximated (J. L. Hill, 2011). As shown in Chipman, George, and McCulloch, 2010, the algorithm tends to find very similar fits with different seeds. Convergence to the fit can be seen in Figure 13 by looking at the draws of  $\sigma$ . The first one-hundred draws in red are burn in, these are not used for the final model.

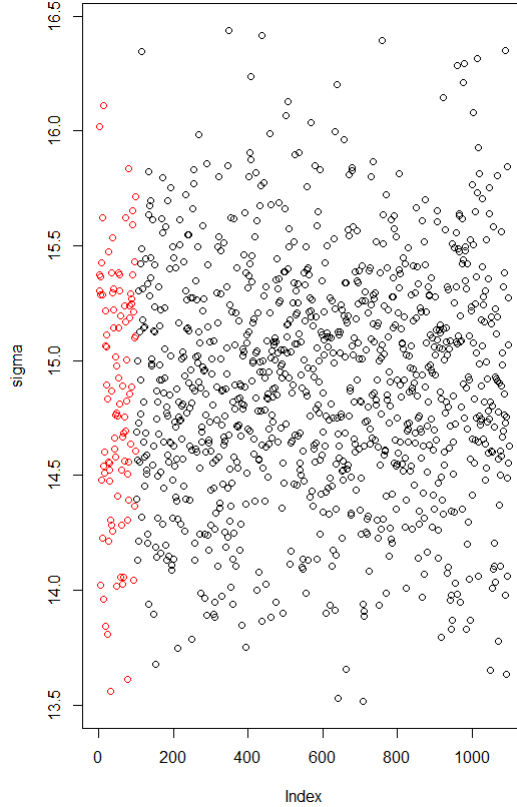


Figure 13: An example of BART convergence. The draws seen in red are the first 100 burn-in draws. These are not included in the final model. The true value of  $\sigma$  was 15. If the model did not converge, the draws of  $\sigma$  would not be homogeneous.

## E.1 Priors

We can write the estimation of  $Y$  as

$$Y \approx \sum_{j=1}^m g(x; T_j, M_j) + \epsilon,$$

where  $T_j$  denote the  $j^{th}$  tree and  $M_j$  denote the  $j^{th}$  vector of terminal nodes,  $M_j = (\mu_{1j}, \mu_{2j}, \dots, \mu_{t_j j})$ . The parameters in the model are then  $(T_j, M_j)$  and  $\sigma$ . The priors are restricted to the form

$$p(M_1, \dots, M_m, T_1, \dots, T_m) \propto \left[ \prod_{j=1}^m p(M_j | T_j) p(T_j) \right] p(\sigma),$$

and

$$p(M_j | T_j) = \prod_{i=1}^{t_j} p(\mu_{ij} | T_j).$$

With this specification the pairs  $(T_j, M_j)$  and  $\sigma$  are a priori independent, making the calculation of the posteriors much easier (Chipman, George, & McCulloch, 2010).

The prior for the trees has three parts:

1. The probability that a node is non-terminal is  $\frac{\alpha}{(1+d)^\beta}$ , where  $d$  is the depth of the node with  $\alpha \in (0, 1)$  and  $\beta \in [0, \infty)$  (The first node has depth 0, second 1, etc). The default values are  $\alpha = 0.95$  and  $\beta = 2$ .
2. The probability that a variable is used at a split is uniform over the remaining predictors.
3. The probability of the splitting value is uniform over the observed values of the variable at the split. A main advantage of this is that it is invariant to monotonic transformations of the response (Chipman, George, & McCulloch, 1998).

The prior used for  $\sigma$  is an inverse chi-squared distribution with degrees of freedom  $\nu = 3$  and scale  $\lambda$  selected such that  $P(\sigma < \hat{\sigma}) = 0.9$ , where  $\hat{\sigma}$  is the residual standard error from a least squares regression of  $y$  on  $(\mathbf{x}, t)$ . The prior for  $\mu_{ij} \mid T_j \sim N(0, \sigma_\mu^2)$  with  $\sigma_\mu^2 = \frac{0.5}{2\sqrt{m}}$ . It should be noted that BART transforms the response so that values range from -0.5 to 0.5 and are centered at zero.

The sampling conditional distribution is the product of the conditional distributions for the  $j^{th}$  tree:

$$\theta_i = (T_i, M_i, \sigma, \mathbf{X}, t),$$

$$p(Y \mid \theta) = \prod_{k=1}^{t_j} \prod_{i=1}^{n_k} f(y_{ki} \mid \theta_k),$$

with

$$y_{k1}, \dots, y_{kn_k} \mid \theta_k \sim N(\bar{\mu}_k, \sigma^2), \quad k = 1, \dots, t_j \text{ for a fixed } j,$$

where  $n_k$  represents the number of responses represented by the  $k^{th}$  terminal node. The posterior is then

$$p((T_1, M_1), \dots, (T_m, M_m), \sigma \mid y)$$

To get samples from the posterior distribution, a Bayesian backfitting MCMC algorithm can be used. It involves  $m$  successive draws from,

$$(T_j, M_j) \mid T_{-j}, M_{-j}, \sigma, y, \quad j = 1, \dots, m,$$

where  $T_{-j}, M_{-j}$  are the trees and parameters for all trees except the  $j$ -th tree. This is followed by a draw of  $\sigma$  from the full conditional,

$$\sigma \mid T_1, \dots, T_m, M_1, \dots, M_m, y.$$

A set of  $Q$  draws (after sufficient burnin) yields  $f_1^*, \dots, f_Q^*$ , which can be used as an approximate sample of size  $Q$  from  $p(f \mid y)$ . This can be used to estimate the conditional mean,

$$\frac{1}{Q} \sum_{q=1}^Q f_q^*(\mathbf{x}, t) \approx E(f(\mathbf{x}, t) \mid y).$$

Similarly, conditional quantile estimates can be obtained by taking the quantiles of  $f_q^*(\mathbf{x}, t)$ .  
 (Chipman, George, & McCulloch, 1998, 2010; J. Hill, Linero, & Murray, 2020)